

# Seasonal thawing of high Arctic soils triggers selective microbial growth and predation

Margaret A. Cramm,<sup>1,2,3</sup> Ömer K. Coskun,<sup>4</sup> Francesco Montemagno,<sup>5</sup> Matteo Selci,<sup>5,6</sup> Daniel S. Read,<sup>7</sup> Tim Goodall,<sup>7</sup> Brianna Green,<sup>8</sup> Sayali A. Mulay,<sup>9,10</sup> Katie Sipes,<sup>9</sup> Andrey A. Abramov,<sup>11</sup> Catherine M. Heppell,<sup>12</sup> Julia Boike,<sup>13,14</sup> Donato Giovannelli,<sup>5,6,15,16,17</sup> Tatiana A. Vishnivetskaya,<sup>9</sup> Robert L. Hettich,<sup>10</sup> Andrew D. Steen,<sup>8,9,18</sup> Karen G. Lloyd,<sup>9,19</sup> William D. Orsi,<sup>4,20</sup> Anne D. Jungblut,<sup>3</sup> James A. Bradley<sup>2,21</sup>

**AUTHOR AFFILIATIONS** See affiliation list on p. 17.

**ABSTRACT** Climate warming threatens Arctic permafrost with seasonal cycles of freezing and thawing. Arctic soil microorganisms regulate carbon stocks and greenhouse gas exchanges with the atmosphere, yet their precise seasonal growth and dormancy dynamics, and their responses to permafrost thaw, are not well understood. We thawed frozen Svalbard active layer soil and traced microbial growth using DNA quantitative stable isotope probing with H<sub>2</sub><sup>18</sup>O. We observed temporal growth patterns resulting in distinct early (21-day) and late-stage (98-day) growing microbial populations. In particular, Acidobacteriota, Actinobacteriota, Bacteroidota, Proteobacteria, and predatory and epibiont bacterial taxa (such as those affiliated to Bdellovibrionota and Patescibacteria) were identified in the soil active layer as clades that were growing following thawing. Methane concentrations in our microcosms remained low, yet *pmoA* genes were <sup>18</sup>O-labeled, indicating growth of aerobic methane-oxidizing bacteria. Approximately half of the microbial taxa detected did not grow, suggesting that Arctic soils constitute sizeable reservoirs of dormant microorganisms. Our results reveal complex and temporal microbial dormancy, growth, death, predation, and parasitism dynamics in seasonally changing Arctic soils. These processes likely regulate the exchange and storage of soil carbon across the increasingly vulnerable Arctic region.

**IMPORTANCE** Microorganisms play key roles in transforming soil carbon into greenhouse gases. As Arctic soils warm as a result of climate change, greater depths and expanses of permanently frozen soil are experiencing seasonal thaw. Despite the importance of active soil microorganisms in transforming soil carbon, the seasonal freezing and thawing of Arctic soils and associated dormancy and re-activation of microbial populations are not well constrained. Here, we thawed and incubated active layer (i.e., seasonally thawing) Arctic soil with a stable isotope to directly label the DNA of growing soil microorganisms. We found that half of the microbial diversity did not grow after thaw and that some groups, including the Bacteroidota and predatory bacteria, grew disproportionately. The growing microbial community shifted over time, and bacteria capable of oxidizing methane grew more after prolonged thaw. These findings highlight that dormancy, predation, and variable growth dynamics are important factors determining ecological and biogeochemical processes in thawing Arctic soil.

**KEYWORDS** Arctic soil, microbial communities, carbon cycle, qSIP, microbial dormancy

Arctic soils contain approximately a third of the global soil carbon (C) pool (1, 2) and are at the forefront of climate change, since air temperatures in the Arctic are warming four times faster than the global average (3). As a consequence, Arctic permafrost is thawing, and the permafrost active layer (which experiences seasonal

**Editor** Emily B. Graham, Pacific Northwest National Laboratory, Richland, Washington, USA

**Peer Reviewers** Bram W. G. Stone, Pacific Northwest National Laboratory, Richland, Washington, USA; Zahra Fatima Islam, The University of Melbourne, Melbourne, Victoria, Australia

Address correspondence to Margaret A. Cramm, m.a.cramm@qmul.ac.uk, or James A. Bradley, jbradley.earth@gmail.com.

The authors declare no conflict of interest.

See the funding table on p. 18.

**Received** 22 May 2025

**Accepted** 19 March 2026

**Published** 7 May 2026

Copyright © 2026 Cramm et al. This is an open-access article distributed under the terms of the [Creative Commons Attribution 4.0 International license](https://creativecommons.org/licenses/by/4.0/).

freezing and thawing) is deepening and exposing vast carbon stocks to microbial degradation (4–6). Permafrost thaw is predicted to release 5%–15% of Arctic soil carbon as carbon dioxide (CO<sub>2</sub>) and methane (CH<sub>4</sub>) by 2100 under the current global trajectory (RCP8.5) (2, 7), causing a 0.13°C–0.27°C increase in global average surface temperature (7).

The production of greenhouse gases from active layer soils and permafrost is a microbially driven process (8, 9). With increasing permafrost thawing depth and duration, soil microorganisms in newly formed active layer soils will be able to degrade a larger source of carbon substrates for longer and potentially at faster rates, thus increasing soil respiration and greenhouse gas emissions to the atmosphere (10).

Microbially mediated transformation of carbon from soils to the atmosphere is dependent on the composition and metabolic capabilities of the organisms inhabiting the soil environment (11, 12), as well as the physico-chemical characteristics of the soil, and the physical and biochemical actions of plants and animals in the soil and on its surface (8, 13–20). Active layer microbial communities exhibit seasonal variations in the relative abundances of certain bacterial phyla (21, 22), with Proteobacteria, Acidobacteriota, Actinobacteriota, and Verrucomicrobiota often found representing dominant portions of the community (22–25). Schostag et al. (26) effectively showed changes in bacterial, fungal, and protozoan responses to thaw in Svalbard active layer soil using RNA sequencing, showing dominance of copiotrophic bacteria in the first 16 days following thaw. This study demonstrated the utility of physiology-based genomic investigations for understanding microbial carbon degradation in Arctic soil. Nevertheless, the seasonal changes in microbial dynamics in Arctic soils, including growth, death, and dormancy, are not well understood, despite the important role that microbial physiology plays in soil carbon turnover and the need to capture and constrain these processes in soil microbial and biogeochemical models (27–31). Pulses of greenhouse gases measured following Arctic soil active layer thawing highlight that the microbial community is quick to respond to thaw, with important consequences on greenhouse gas fluxes from Arctic terrestrial environments (32). However, despite the critical connection between active layer soil microorganisms and the global carbon budget, we lack data on the precise population dynamics and microbe-associated carbon transformations in Arctic active layer soils following thawing due to seasonal changes.

Quantitative DNA stable isotope probing (qSIP) with H<sub>2</sub><sup>18</sup>O is an effective physiology-based genomic method for measuring taxon-specific growth, death, and dormancy (33). qSIP has clarified microbial growth dynamics in experimentally warmed tundra soils, showing that the length of warming (months versus decades) affects clade-specific microbial growth and bacterial growth rates (34). qSIP was further used to reveal taxon-specific growth rates of experimentally warmed Antarctic glacial forefield soils that were sensitive to successional stage and local vegetation (35).

To understand the changes in microbial community dynamics, including the growth and activity of microorganisms in active layer soil following thaw, we conducted *ex situ* incubations of subsurface active layer soils from Svalbard, in the high Arctic, one of the regions presently facing the fastest rates of warming on Earth (36, 37). Our aim was to identify growing and non-growing microorganisms in active layer soil at two time points following thaw (21 and 98 days) and to identify associated taxon-specific changes in microbial community growth.

## MATERIALS AND METHODS

### Study site and sample collection

Our study site, the Bayelva Permafrost Monitoring Observatory near Ny-Ålesund (78.921078° N, 11.857037° E), is situated on the Brøggerhalvøya peninsula in northwest Svalbard. The area is warmed by the North Atlantic's West Spitsbergen Current and has an average air temperature range of –17.0°C to –3.8°C in January and 4.6°C to 6.9°C in July (between 1993 and 2011) (38). The Bayelva area is underlain by continuous

permafrost that is ~100 m thick, and the depth of the active layer is 1 to 2 m (38). The site is covered in bare non-sorted circles of 1 m diameter, surrounded by rims hosting grasses, sedges, lichens, and moss (38), and the soil is of mineral type (13). In 2021, the year of sampling, the range of temperature of the soil at a depth of 21 cm was  $-4.8^{\circ}\text{C}$  to  $9.1^{\circ}\text{C}$ , with 104 continuous days of temperatures above  $0^{\circ}\text{C}$  in 2021 and 59 continuous days above  $4^{\circ}\text{C}$  (Fig. 1B).

On 25 March 2021, we extracted a single frozen core from the soil surface to 2.4 m depth from Bayelva Permafrost Monitoring Observatory near Ny-Ålesund ( $78.921078^{\circ}\text{N}$ ,  $11.857037^{\circ}\text{E}$ ) (Fig. 1) using a dry borehole method as described in Shi et al. (40). We subsampled subsurface active layer soil from this core, extracting soil from a depth corresponding to 18–27 cm below the soil surface. We transferred the loose, mixed material into sterile Whirl-Pak bags and stored them at  $-20^{\circ}\text{C}$  for 3 months before incubation at  $4^{\circ}\text{C}$  to simulate seasonal thawing. Methods for obtaining soil moisture, organic matter content, and cell abundance from the soil core are described in the Supplemental Methods. On 18 June 2022, we collected soil from a nearby 35 cm excavated rectangular soil pit ( $78.921367^{\circ}\text{N}$ ,  $11.865867^{\circ}\text{E}$ ) (41) that maintained an intact wall. We stored this soil in a Whirl-Pak bag at  $-20^{\circ}\text{C}$  until analyses. This soil was analyzed for trace element concentrations to serve as a general reference for the geochemical characteristics of soils at the Bayelva site. Methods for obtaining trace element data from the soil pit are described in the Supplemental Methods.

### Microcosm set-up

To create microcosms of thawing active layer soil, we thawed soil collected from 18 to 27 cm depth of the frozen core at room temperature and immediately placed 2 g of soil into autoclaved 20 mL glass vials on ice. We added 1 mL of either heavy water containing the 97%  $^{18}\text{O}$  isotope of oxygen ( $\text{H}_2^{18}\text{O}$ ), or water of natural isotopic composition ( $\text{H}_2^{16}\text{O}$ , ultra-pure Milli-Q water, autoclaved and filter-sterilized through a 0.2  $\mu\text{m}$  pore-size filter). Microorganisms growing in the presence of  $\text{H}_2^{18}\text{O}$  incorporate  $^{18}\text{O}$  into newly synthesized DNA molecules at a rate equivalent to DNA incorporation of  $^{16}\text{O}$  from  $\text{H}_2^{16}\text{O}$  (42). The headspace in each individual vial after the addition of soil and water was approximately 18 mL. We created 10 replicate microcosms: 5 intended for a 21 day incubation and 5 for a 98 day incubation. In 2021, soil from this site and depth was above  $0^{\circ}\text{C}$  for 104 days; thus, the longer 98 day incubations correspond roughly to the duration of seasonal thawing. Eight replicate microcosms (four for the 21 day incubation and four for the 98 day incubation groups) received water of standard (untreated) isotopic composition ( $>99\%$   $\text{H}_2^{16}\text{O}$ ). Two replicate microcosms (one for each of the 21 and 98 day incubation groups) received  $\text{H}_2^{18}\text{O}$ . The microcosm replication for DNA SIP methodology was aligned with established methods (43). The water content of the 2:1 wt/vol ratio slurries contained 81%  $^{18}\text{O}$  isotope due to the dilution of the  $\text{H}_2^{18}\text{O}$  with natural soil moisture. This led to a five times increase in soil moisture in microcosms compared to the soil moisture of the collected soil, which is slightly higher than the typical three times soil moisture increase that occurs seasonally *in situ* as soils thaw during late spring/early summer (44). We sealed vials with butyl stoppers and exchanged the headspace with standardized zero-grade air (21%  $\text{O}_2$  with  $\text{N}_2$  balance, 0%  $\text{CH}_4$ , 0%  $\text{CO}_2$ ). We created parallel anoxic microcosms exactly as above; the headspaces of these were flushed with zero-grade  $\text{N}_2$  gas. Microcosms were incubated at  $4^{\circ}\text{C}$  in the dark for 21 or 98 days. Following incubation, vials were frozen at  $-20^{\circ}\text{C}$ .

### Headspace gas measurement

$\text{CO}_2$ ,  $\text{CH}_4$ , and nitrous oxide ( $\text{N}_2\text{O}$ ) were measured using gas chromatography with electron capture and flame ionization detection (Agilent Technologies 7890B GC system). For each measurement, 250  $\mu\text{L}$  of air was removed (without replacement) from the headspace of incubation vials using a flame-sterilized gas-tight syringe and manually injected. Headspace gas was sampled on 0, 7, 14, 21, 28, 49, 77, and 98 days of incubation. A six-point calibration curve was created each day of gas measurement from a

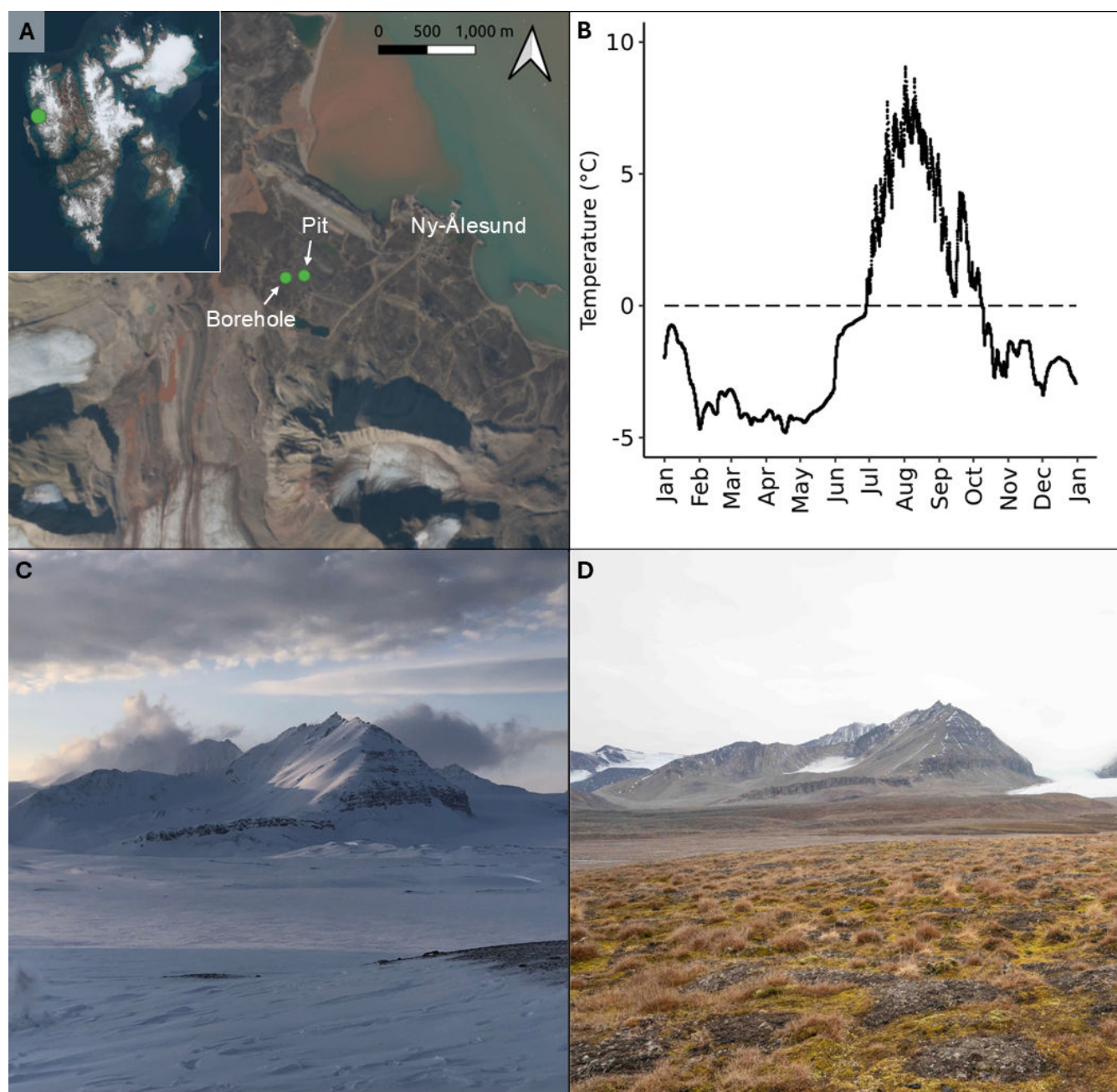


**FIG 1** Location, annual soil temperature, and photographs of the Bayelva Permafrost Monitoring Observatory near Ny-Ålesund, Svalbard. (A) Map showing the location of the core borehole (78.921078° N, 11.857037° E) and the soil pit (78.921367° N, 11.865867° E). Map data were obtained from the Norwegian Polar Institute. (B) Soil temperature at the Bayelva Permafrost Monitoring Observatory near Ny-Ålesund, Svalbard, at 21 cm depth from 1 January 2021 to 2 January 2022. Soil temperature data are from Boike et al. (39) and correspond to soil temperature at 21 cm beneath the soil surface. The dashed horizontal line indicates 0°C. The seasonal characteristics of the ground near the observatory can be seen in panels C and D. Pictures were taken in (C) March 2022 and (D) September 2022 by Margaret Cramm.

dilution series of calibration gas consisting of 100 ppm of CH<sub>4</sub>, 100 ppm of N<sub>2</sub>O, and 3,700 ppm of CO<sub>2</sub>. The headspace gas was not replaced during the incubation.

O<sub>2</sub> was optically measured using a Fibox 4 Stand-alone Fiber Optic Oxygen Meter (PreSens Precision Sensing). Ethanol-sterilized 5 mm Planar Oxygen-Sensitive sensor spots (PreSens Precision Sensing GmbH) were mounted on the inside of three of five

replicate vials before the incubation and prior to adding soil. O<sub>2</sub> was measured (non-destructively) at least five times per week during the incubation.

### DNA extraction

DNA was extracted from vials as described in Coskun et al. (45) and further described in the Supplementary Methods. We purified the concentrated lysate using the Qiagen DNeasy PowerClean Pro Cleanup kit according to the manufacturer's instructions and eluted the DNA in 100  $\mu$ L. DNA was quantified using the fluorometric Qubit dsDNA HS Assay (Thermo Scientific) following the manufacturer's instructions. DNA for unfractionated 16S rRNA gene amplicon sequencing libraries was diluted 1:1,000 with PCR-grade water to dilute PCR inhibitors that prevented PCR amplification of DNA in the eluted extraction, and in 1:10 and 1:100 dilutions. DNA for fractionation was not diluted prior to fractionation because this protocol diluted the DNA  $\sim$ 1:1,000. Two negative-control DNA extractions were done without soil or slurry added to the extraction mixture to assess potential levels of contamination.

### DNA fractionation

We fractionated DNA from the microcosm that received H<sub>2</sub><sup>18</sup>O and a corresponding microcosm that received H<sub>2</sub><sup>16</sup>O using density gradient centrifugation according to described DNA stable isotope probing methods (33, 45, 46). For three technical triplicates, 25  $\mu$ L of DNA template was added to  $\sim$ 3.3 mL of cesium chloride (CsCl)-gradient buffer solution to a final density of 1.7 g mL<sup>-1</sup> in 3.3 mL OptiSeal polyallomer tubes (Beckman Coulter). These tubes were centrifuged at 65,000 rpm for 72 h at 18°C in a TLN-100 Optima MAX-TL ultracentrifuge (Beckman Coulter) to create a density gradient. The density gradient was separated into 20 fractions (165  $\mu$ L) within 3 h of centrifugation using a syringe pump and fraction recovery system as described in Coskun et al. (45) and in the video description in Cramm (47). The density of each fraction was inferred according to a linear density model based on the measured density of seven or eight fractions using an AR200 digital refractometer (Reichert Analytical Instruments). Fraction densities are shown in Fig. S1. We precipitated DNA from the density gradient using 2  $\mu$ L glycogen (10 mg mL<sup>-1</sup>) and two volumes of filter- and UV-sterilized 30% polyethylene glycol 6000 solution (45, 46) and resuspended it in 30  $\mu$ L PCR-grade water.

### Quantitative PCR (qPCR)

We quantified 16S ribosomal RNA (rRNA) genes from fractionated and unfractionated DNA with qPCR using the 515F-Y (5'-GTGYCAGCMGCCGCGGTAA-3') and 806R (5'-GGAC-TACNVGGGTWCTAAT-3') primers (48, 49). The qPCR reaction mixture (20  $\mu$ L) was dispensed using an epMotion 5070 pipetting robot (Eppendorf) and was composed of 4  $\mu$ L template DNA, 0.4  $\mu$ L of each primer (10  $\mu$ M), 5.2  $\mu$ L PCR-grade water, and 10  $\mu$ L SsoAdvanced Universal SYBR Green Supermix (Bio-Rad). The PCR protocol was as follows: an initial denaturation at 95°C for 3 min, followed by 40 cycles of denaturation at 95°C for 10 s, followed by annealing and elongation at 55°C for 30 s, followed by fluorescence detection (CFX Connect real-time PCR system; Bio-Rad). qPCR reactions containing no template DNA were included in all reactions, and only samples for which the starting quantity (SQ) was more than the SQ for the "no-template" reaction were retained. Only qPCR runs with efficiency >90% and <110%, and  $R^2 > 0.87$ , were retained.

We also quantified *pmoA* genes from fractionated and unfractionated DNA with qPCR using the A189F (5'-GGNGACTGGGACTTCTGG-3') and Mb661R (5'-CCGGMGCAACGTCYT-TACC-3') primers (50), and *mcrA* genes from unfractionated DNA using the mlas (5'-GGTGGTGMGGDTTCACMCARTA-3') and *mcrA*-rev (5'-CGTTCATBGCCTAGTTVGGR-TAGT-3') primers (51). The qPCR reaction mix was the same as for qPCR of the 16S rRNA genes. The protocol for *pmoA* amplification was an initial denaturation at 94°C for 3 min, followed by 40 cycles of denaturation at 94°C for 30 s, annealing at 56°C for 40 s, and elongation at 72°C for 1 min, followed by fluorescence detection (StepOnePlus Real Time System, Applied Biosystems). The efficiency of the *pmoA* qPCR amplification was

between 90 and 117% and  $R^2$  values were between 0.91 and 0.99. The protocol for *mcrA* amplification was an initial denaturation at 95°C for 3 min 30 s, followed by 40 cycles of denaturation at 95°C for 30 s, annealing at 55°C for 45 s, and elongation at 72°C for 30 s, followed by fluorescence detection (StepOnePlus Real Time System, Applied Biosystems). The efficiency and  $R^2$  for *mcrA* gene qPCR were 99% and 0.998, respectively.

### 16S rRNA gene sequencing and analysis

The V4 region of the 16S rRNA genes was amplified with polymerase chain reaction (PCR) using the 515F and 806R primers (48, 49). Triplicate PCR reactions were done using a touchdown protocol described in Cramm et al. (52) and further described in the Supplementary Methods. Negative PCR controls, in which no template DNA was added to the PCR reaction, were used to determine contamination during PCR. Negative DNA extraction controls and negative PCR controls were also prepared for sequencing to determine contamination. Triplicate PCR reactions were pooled and cleaned using AppMag PCR Clean Up Beads (Appleton) according to the manufacturer's instructions. Equal moles of the pooled amplicons were sequenced on an Illumina MiSeq PE250 (2 × 250 bp) by the sequencing facility at the Natural History Museum (London, UK). 16S rRNA gene amplicon sequences can be found in the NCBI Sequence Read Archive under the BioProject accession [PRJNA1118335](https://www.ncbi.nlm.nih.gov/bioproject/PRJNA1118335).

Amplicon sequence variants (ASVs) were used for taxonomic community analysis. Adapters were removed from paired-end reads using Cutadapt version 4.0 (53), and reads shorter than 150 bp were discarded. We created ASVs using DADA2 version 1.16.0 (54, 55). We discarded reads with expected errors above 2. Forward and reverse reads were truncated to 250 bp and 200 bp, respectively, and reads shorter than these were discarded. The median library size was 51,343 reads (Fig. S2). Taxonomy was assigned using an RDP Naive Bayesian Classifier algorithm and the SILVA v.138.1 sequence database (56, 57). Taxonomic names may differ from other sequence databases or published names (58). Diversity and statistical analysis were performed in R version 4.3.2 (59) using the packages vegan version 2.6-4 (60) and phyloseq version 1.46.0 (61). There were 2,666 ASVs in the data set with 40 singleton ASVs and 97 doubleton ASVs. We retained singletons and doubletons, and data were rarefied to 10,000 reads prior to alpha diversity calculations using Chao1 and Inverse Simpson indices. Indices were calculated based on the mean of 10 iterations. Diversity index data were evaluated for normality using the Shapiro-Wilk normality test ( $\alpha = 0.05$ ). Significance between the difference of means of normal diversity index data was determined using a Welch two-sample *t*-test ( $\alpha = 0.05$ ). Data were not rarefied, but they were transformed to relative sequence abundance for beta diversity calculations using Bray-Curtis distance matrix and visualization of 16S rRNA gene sequence community composition. The ANOSIM test (999 permutations,  $\alpha = 0.05$ ) was performed on the distance matrix to determine similarity of the different incubation groups.

### Estimating $^{18}\text{O}$ enrichment of 16S rRNA genes

We calculated  $^{18}\text{O}$ -atom fraction excess (AFE) values according to methods described in Hungate et al. (33) and Coskun et al. (45, 62) using the HTSSIP package in R (63). For each technical replicate, AFE was calculated at the ASV level by the difference in density between the ASV in the  $\text{H}_2^{16}\text{O}$  control microcosm and its density in the corresponding  $\text{H}_2^{18}\text{O}$  microcosm. Only those ASVs that increased in density with 90% confidence after 1000 bootstraps and for which the lower confidence interval did not overlap zero were considered to have incorporated the  $^{18}\text{O}$ -label into their DNA. Negative labeling, in which the AFE is below 0 with a 90% confidence interval, occasionally arises due to density variability in rare ASVs (64) and can be disregarded. The technical replicates of the controls were analyzed separately to capture variability in the fractionating procedure. Due to a single technical replicate of the 98 day  $\text{H}_2^{16}\text{O}$  control group failing fractionation, only two technical  $\text{H}_2^{16}\text{O}$  control replicates were used to calculate AFE for the 98 day incubation. This may have caused wider 90% confidence intervals for the 98 day AFE

values and therefore a possible increase in the number of ASVs showing a false negative result for  $^{18}\text{O}$ -labeling.

## RESULTS AND DISCUSSION

### Site and soil characteristics

We collected an active layer soil sample from near the Bayelva Permafrost Monitoring Observatory site (78.921078° N, 11.857037° E) near Ny-Ålesund, Svalbard (38, 39). The characteristics of subsurface active layer soil (from 18 to 27 cm depth) near the Bayelva Permafrost Monitoring Observatory are shown in Table S1. Soil moisture was 10.3%, soil organic matter was 2.5% dry weight, and the soil contained  $10^6$  cells per g of wet soil and 45 ng DNA per g of wet soil. The concentrations of selected trace elements are shown in Table S1. Fe was abundant ( $2.3 \times 10^5$  mg  $\text{kg}^{-1}$ ), while other biologically relevant trace metals such as Co, Ni, Cu, and Zn were present at  $<50$  mg  $\text{kg}^{-1}$ . Mg was present at 4,580 mg  $\text{kg}^{-1}$ , and Mn was present at 478 mg  $\text{kg}^{-1}$ .

### Microbial respiration upon thaw

$\text{CO}_2$  concentrations in the microcosms increased within days following thaw and incubation at 4°C and continued to increase during the first 28 days (22.0 mmol  $\text{g}^{-1}$   $\text{day}^{-1}$ ) (Fig. S3A). This indicates that soil microorganisms rapidly resumed activity following thaw, and that Arctic soil carbon budgets and greenhouse gas fluxes may be highly sensitive to episodic winter warming events with sustained positive-degree temperatures (65). We reason that the increased availability of liquid water (from thawing of soil ice to soil water, as well as added  $\text{H}_2^{16}\text{O}$  or  $\text{H}_2^{18}\text{O}$ ) was the primary trigger for the rapid onset of microbial respiration and  $\text{CO}_2$  release following soil thaw (as discussed by Nikrad et al. [9]).  $\text{CO}_2$  concentrations in the headspace of incubation vials continued to increase beyond 28 days in two of five replicates (15.2 nmol  $\text{g}^{-1}$   $\text{day}^{-1}$ ) and decreased or plateaued after 28 days in three replicates, suggesting that community-level growth ceased or slowed after 28 days in these microcosms (Fig. S3A).

Methane concentrations remained low and stable (near 2 nmol  $\text{g}^{-1}$  of soil) during the incubation (Fig. S3C), suggesting either (i) no substantial methane production or consumption in the thawed soil or (ii) a steady-state level of methane production and consumption. The headspace of our microcosms remained oxic throughout the incubation (Fig. S3B), which may have inhibited methanogenesis. We also carried out parallel anoxic incubations of active layer soil, which did not produce substantial increases in methane concentrations either (Fig. S4B). The minimal production of methane under anoxic headspace is consistent with prior studies of thawed Svalbard soils and could be attributed to low organic matter content of the soil (1.38% by weight) and also relatively high iron concentrations in the soil (Table S1) which promotes iron reduction in anoxic conditions and can suppress methanogenesis (24, 66).

### “Early” and “late” communities

We detected microbial growth in the microcosms that were terminated after 21 days of incubation (Fig. 2). DNA extracted from soils that were incubated with  $\text{H}_2^{18}\text{O}$  water was enriched in  $^{18}\text{O}$  (hereafter “ $^{18}\text{O}$ -labeled” DNA) relative to DNA extracted from soils incubated with  $\text{H}_2^{16}\text{O}$  (Fig. 2). At 21 days, a substantial portion (~30 to 45%) of the DNA in  $\text{H}_2^{18}\text{O}$ -amended microcosms remained unlabeled, indicating that a portion of the community did not grow and presumably remained dormant during the initial incubation period (Fig. 2A). We observed a shift to a heavier density range at the end of the incubation (i.e., at 98 days; Fig. 2B, yellow lines), indicating that microbial growth continued between 21 and 98 days. Despite continued growth from 21 to 98 days (Fig. S5B), 16S rRNA gene copy number did not increase during the incubation (Fig. S6C), suggesting that either early-growing cells replaced and destroyed dead or dormant cells or that some previously dormant cells started growing after 21 days.

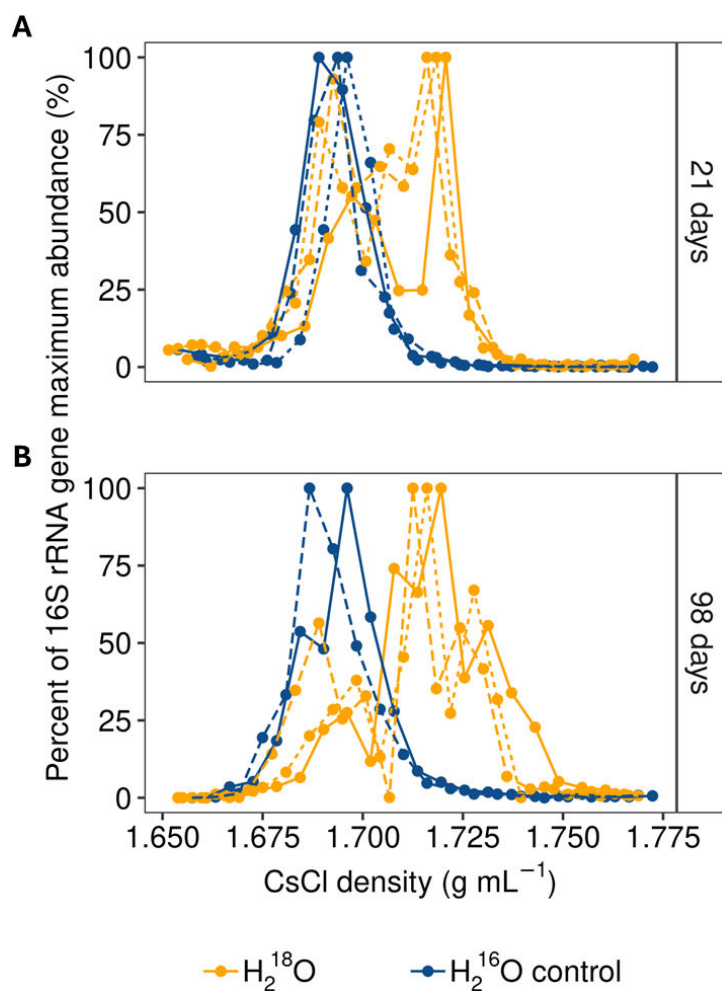


**FIG 2** Density of DNA extracted from  $\text{H}_2^{18}\text{O}$ -amended and  $\text{H}_2^{16}\text{O}$  control microcosms. The abundances of 16S rRNA genes at different buoyant densities measured with qPCR at (A) 21 and (B) 98 days in oxic conditions are shown. Blue lines show the abundance of 16S rRNA genes in DNA extracted from the control microcosms that received  $\text{H}_2^{16}\text{O}$  water (i.e.,  $\text{H}_2^{16}\text{O}$  control). The yellow lines show the abundance of 16S rRNA genes in DNA extracted from the microcosms that received  $\text{H}_2^{18}\text{O}$  water. The solid and dashed lines correspond to technical replicates. The y-axis values represent the percent of the 16S rRNA gene abundances normalized to the maximum value within the same replicate.

The overall composition of the total microbial communities present at the “early” and “late” incubation time points was similar. ASV richness and evenness (as determined by Chao1 and inverse Simpson indices) and total abundance (as determined by qPCR of 16S rRNA genes) did not significantly change over the 98 day incubation (Fig. S6A through C), and at a phylum level, the composition of the initial (i.e., pre-thaw), 21 day, and 98 day microbial communities was generally similar (Fig. 3A and B and 4A and B) and did not differ statistically (community composition based on Bray-Curtis Dissimilarity Index of the 21 and 98 day microbial communities, ANOSIM,  $R = 0.15$ ,  $P = 0.5$ ).

### Taxon-specific growth following thaw

Microorganisms grew in thawed soils during the first 21 days and continued to grow during the 21 to 98 day incubation period (Fig. 2; Fig. S5). We observed taxon-specific differences in the growing portion of the 21 and 98 day communities which were not indicated in diversity index and community compositional comparisons of the total communities. In general, the microbial groups that were most relatively abundant at

21 and 98 days were also those that were labeled with  $^{18}\text{O}$  and therefore detected as growing (Fig. 3 and 4). Sequences attributed to Acidobacteriota, Actinobacteriota, and Proteobacteria collectively comprised  $68\% \pm 3\%$  (21 days) and  $59\% \pm 1\%$  (98 days) of the relative sequence abundance (Fig. 3B and 4B). These phyla also comprised 59% and 55% of the growing ASVs at 21 and 98 days, respectively (Fig. 3C and D and 4C and D). Acidobacteriota, Actinobacteriota, and Proteobacteria are commonly found to be dominant in permafrost-affected soils (24, 25, 35, 67). We also found that many of the ASVs belonging to these dominant groups did not grow, even after 98 days, indicating variable growth and dormancy responses between and within phyla after thaw.

While the overall composition of the total active layer “early” (21 day) and “late” (98 day) communities was similar, the growing members at 21 and 98 days were distinct from each other. Only 22% of ASVs that were  $^{18}\text{O}$ -labeled at 21 or 98 days were  $^{18}\text{O}$ -labeled at both time points. Observed richness (measured by unique ASV abundance) of  $^{18}\text{O}$ -labeled Acidobacteriota, Bacteroidota, Firmicutes, Gemmatimonadota, Myxococcota, Planctomycetota, Proteobacteria, and Verrucomicrobiota increased from the “early” to “late” communities (Fig. 3D and 4D), suggesting that the factors that triggered and supported the growth of members of these phyla persisted or were enhanced during the later stages of the incubation. This is in agreement with previous work showing increases in the relative abundance of Bacteroidota and Verrucomicrobiota species between the beginning (June) and end (October) of the thaw season in soils surrounding Ny-Ålesund, Svalbard (68). Gemmatimonadota, Planctomycetota, and Verrucomicrobiota are generally considered to be “slow growing” (i.e., with doubling times of days to weeks) (69, 70). The ability of a microbial cell to rapidly resume metabolic activity following dormancy, as indicated here by  $\text{CO}_2$  production within days of soil thawing, may suit organisms in habitats that frequently experience fluctuating environmental conditions (71–73). Slow growth is also favored by organisms residing in harsh environments (74–76). ASVs affiliated with Bdellovibrionota, Abditibacteriota, Armatimonadota, and Crenarchaeota were only  $^{18}\text{O}$ -labeled in the “late” communities (and not in the “early” communities) and thus only grew after a longer period of thaw, indicating that the duration of thaw shapes the growth response of the soil microbial community.

Dominant groups in the “early”- and “late”-growing communities may be influenced by nutrient availability and turnover. Actinobacteriota, Bacteroidota, and Proteobacteria, which are prominent in the “early”-growing community, are associated with efficient necromass recycling (77) and may benefit from necromass released from frozen soil upon thaw (78). Moreover, groups broadly associated with the degradation of complex and specific carbon sources were more prominent in the “late”-growing community, including the Armatimonadota, Verrucomicrobiota, and Planctomycetota (79). These groups may be more competitive following the exhaustion of labile carbon sources by “early” growers (80). The disappearance of “early”  $^{18}\text{O}$ -labeled ASVs by 98 days (Methylomirabilota, Thermoplasmotota, Entotheonellaeota, Latescibacterota, Nitrospirota, and Desulfobacterota) could be attributed to the turnover of these groups, potentially due to predation (see “Epibiont and predatory phyla”) or cell death and subsequent degradation of the cellular DNA.

Bacteroidota, despite their low relative 16S rRNA gene abundance (0.8%–2.7% and 9.1%–14.0% at 21 and 98 days, respectively), were disproportionately  $^{18}\text{O}$ -labeled, and all ASVs affiliated with Bacteroidota were  $^{18}\text{O}$ -labeled at 98 days (Fig. 4C). Bacteroidota ASVs grew during the “early” stage, and their growth was sustained in the “late” stage, with AFE of this group increasing by 0.16 between 21 and 98 days (Fig. S7). Some of these ASVs were the most isotopically enriched ASVs in the entire soil community (Fig. 3C and 4C). Overall, this suggests that the growth of Bacteroidota may play a predominant role in post-thaw microbial dynamics despite their relatively low abundance. Bacteroidota are widespread in soil (81) including in Svalbard active layer soils (26). They are competitive degraders of complex carbohydrates owing to efficient and substrate-specific enzyme production and a phylum-specific secretion system that provides gliding motility used

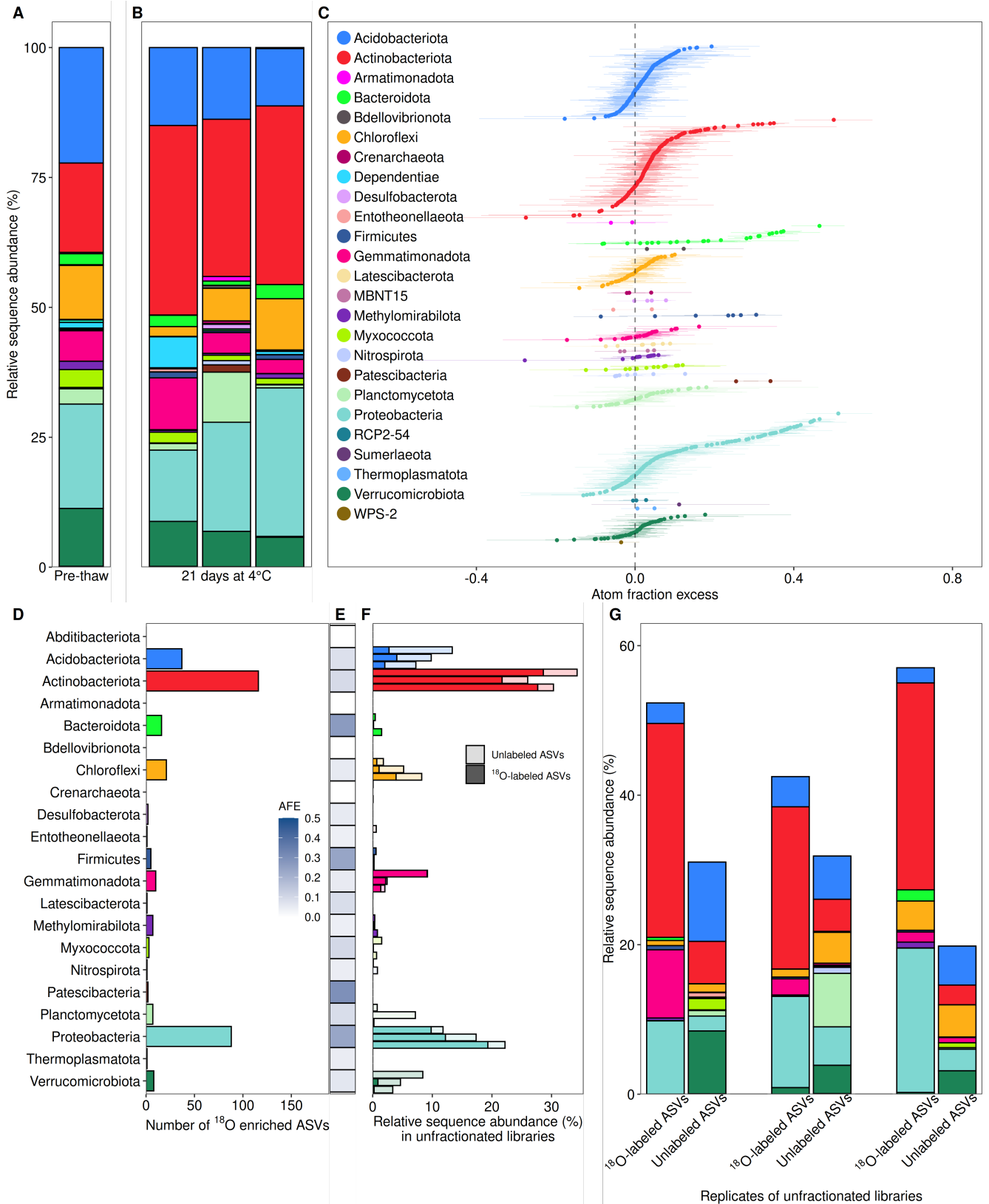


**FIG 3** The composition of the <sup>18</sup>O-labeled and unlabeled microbial community members after 21 days of incubation at 4°C under oxic conditions. (A) Relative 16S rRNA gene sequence abundance of phyla in frozen soil prior to incubation and thaw. (B) Relative 16S rRNA gene sequence abundance of phyla in soil after 21 days of incubation at 4°C. Bars show the community composition of triplicate microcosms. (C) AFE of <sup>18</sup>O in DNA of ASVs. ASVs detected by qSIP (Continued on next page)

Downloaded from https://journals.asm.org/journal/mSystems on 24 June 2026 by 192.171.199.129.

Fig 3 (Continued)

(represented by colored dots) are grouped and colored by phylum and ordered along the y-axis by increasing AFE. Each dot represents the median AFE values, and error bars indicate the 90% confidence intervals. The further an ASV "dot" is to the right, the more enriched that ASV's DNA is in  $^{18}\text{O}$ . AFE shows the magnitude of  $^{18}\text{O}$  incorporation into the DNA of growing microorganisms. (D) The number of ASVs that are enriched in  $^{18}\text{O}$  at 21 days. (E) Mean AFE values of  $^{18}\text{O}$ -labeled ASVs within each phylum. (F) The relative sequence abundance of  $^{18}\text{O}$ -labeled (darkly shaded) and unlabeled (lightly shaded) ASVs of each phylum. Only phyla to which at least one  $^{18}\text{O}$ -labeled ASV belongs (at 21 or 98 days) are shown. Bars show the abundance in triplicate microcosms. (G) The relative 16S rRNA gene sequence abundance of  $^{18}\text{O}$ -labeled and unlabeled ASVs in the unfractionated libraries of replicate microcosms. Seventeen to 26% of the relative sequence abundance of the unfractionated libraries was not detected in the fractionated 21 day qSIP libraries. We attribute this "not detected" ASV abundance to community differences between biological replicates, and it is inherent in the qSIP method, which relies on comparison between biological replicates to determine AFE. The  $^{18}\text{O}$  incorporation status of ASVs of this "not detected" fraction cannot be determined, and so the relative abundances of these are not shown in the plot.

for substrate foraging and tethering of enzymes for concentrating substrate-degrading activity near the cell (82).

### Epibiont and predatory phyla

Members of phyla often associated with predation in soil, including Myxococcota, Patescibacteria, and Bdellovibrionota, were  $^{18}\text{O}$ -labeled following thaw (Fig. 3C and 4C). Myxococcota prey on other bacterial cells (83) and have been implicated as key bacterial predators in permafrost-affected environments (34, 84), owing to their broad host range (85). Patescibacteria (all belonging to the class Saccharimonadia) and Bdellovibrionota (including *Oligoflexia* spp., *Bacterioivora* sp., *Bdellovibrio* sp., and *Silvanigrella* sp.) also grew following thaw (Fig. 3C and 4C). Saccharimonadia are obligate epibionts, growing while attached to surfaces of hosts (86, 87), and show host specificity to members of the Bacteroidota and Actinobacteriota (87, 88). Bdellovibrionota are also known predatory bacteria (89–92). Despite making up <1% of the total relative sequence abundance (Fig. 4B), all detected ASVs of Patescibacteria were  $^{18}\text{O}$ -labeled and growing. Similarly, all detected ASVs of Bdellovibrionota, making up just  $2 \pm 1\%$  of relative sequence abundance, were  $^{18}\text{O}$ -labeled after 98 days. These phyla, while low in relative abundance, were the most  $^{18}\text{O}$ -labeled groups by 98 days, potentially as a result of the consumption of  $^{18}\text{O}$ -enriched hosts and prey, as well as  $^{18}\text{O}$ -labeled water incorporation during growth. Observations indicate that obligately predatory bacteria are >60% more active than their non-predatory counterparts when new carbon sources become available (93), as is likely to occur when soil thaws, which may contribute to the high AFE of predatory phyla observed here. Notably, the AFE of ASVs affiliated to Bdellovibrionota and Patescibacteria present at both 21 and 98 days increased by a mean value of 0.46 and 0.16, respectively (Fig. S7), suggesting continued growth and predation or epibiosis for ASVs belonging to these phyla during sustained thaw. In contrast, ASVs affiliated to Myxococcota decreased in AFE on average over this time, suggesting that turnover may differ between different predatory groups, potentially depending on the growth cycles of prey or host bacteria. While the Myxococcota host range is broad, the Bdellovibrionota host range is narrower (85), and Bdellovibrionota growth may depend more strongly upon prior growth of their host species, contributing to their later  $^{18}\text{O}$ -labeling and growth seen here. The growth dynamics of prey species may additionally affect the timing of predatory activity. Specifically, prey can use dormancy and slow growth as predator-avoidance strategies (94–97).

### Methanotrophic organisms

Methane concentrations remained low during the incubations (Fig. S3C), and we did not detect any 16S rRNA genes that could be attributed to members of the methanogen-affiliated Euryarchaeota or Halobacterota, or any *mcrA* genes indicative of methanogenesis biosynthetic pathways. We measured an isolated increase in methane in a single measurement from a single microcosm (Fig. S3C). This isolated increase was not consistent with the overall trend of methane concentrations, nor did it co-occur with a

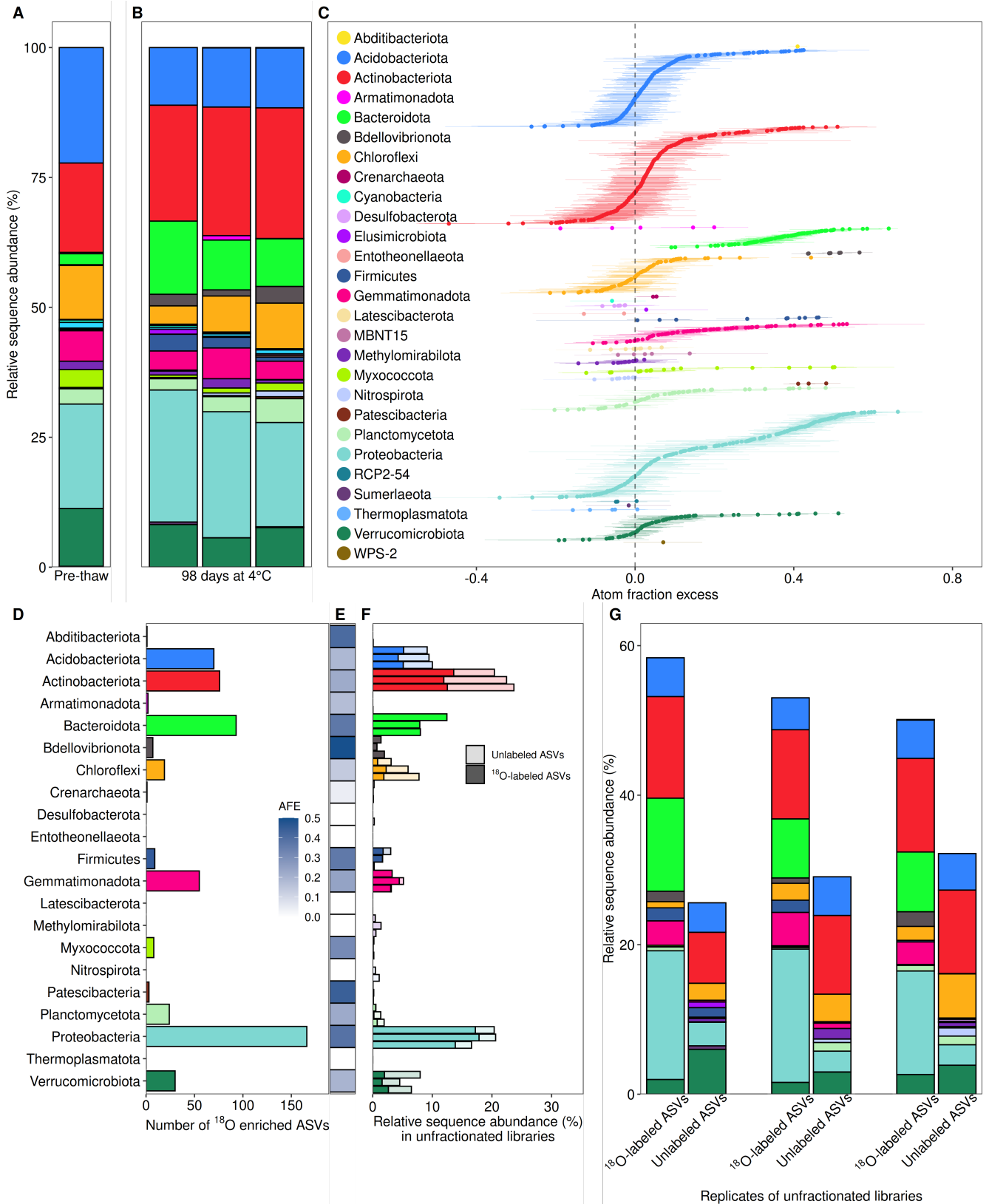


**FIG 4** The composition of the <sup>18</sup>O-labeled and unlabeled microbial community members after 98 days of incubation at 4°C under oxic conditions. (A) Relative 16S rRNA gene sequence abundance of phyla in frozen soil prior to incubation and thaw. (B) Relative 16S rRNA gene sequence abundance of phyla in soil after 98 days of incubation at 4°C. Bars show the community composition of triplicate microcosms. (C) AFE of <sup>18</sup>O in DNA of ASVs. ASVs detected by qSIP (Continued on next page)

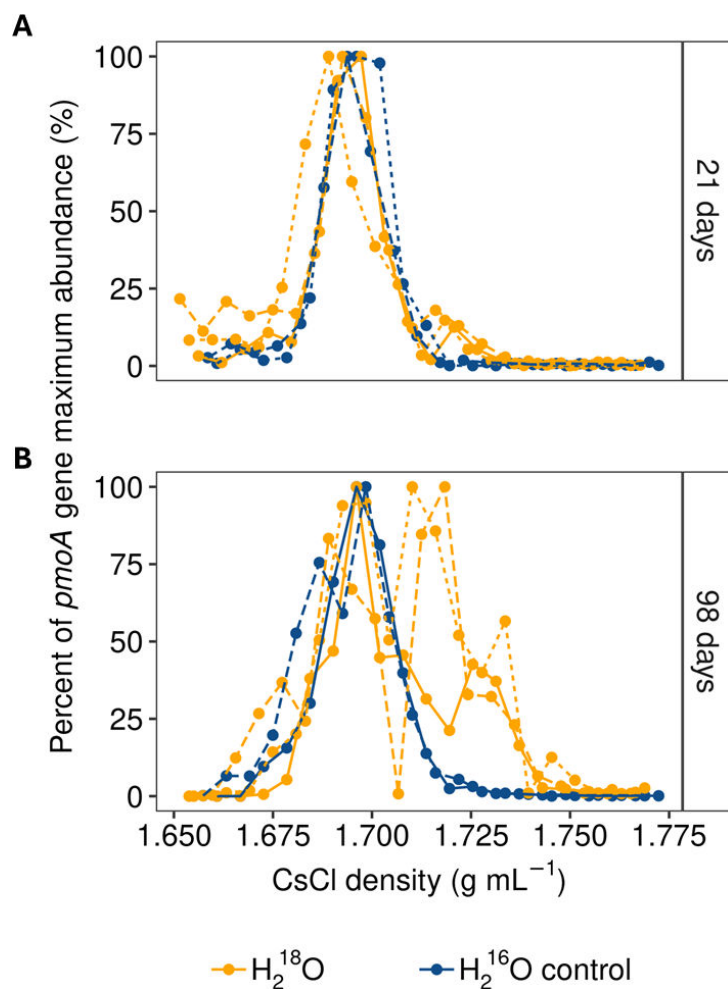
Downloaded from https://journals.asm.org/journal/mSystems on 24 June 2026 by 192.171.199.129.

Fig 4 (Continued)

(represented by colored dots) are grouped and colored by phylum and ordered along the y-axis by increasing AFE. Each dot represents the median AFE values, and error bars indicate the 90% confidence intervals. The further an ASV "dot" is to the right, the more enriched that ASV's DNA is in  $^{18}\text{O}$ . AFE shows the magnitude of  $^{18}\text{O}$  incorporation into the DNA of growing microorganisms. (D) The number of ASVs that are enriched in  $^{18}\text{O}$  at 98 days. (E) Mean AFE values of  $^{18}\text{O}$ -labeled ASVs within each phylum. (F) The relative sequence abundance of  $^{18}\text{O}$ -labeled (darkly shaded) and unlabeled (lightly shaded) ASVs of each phylum. Only phyla to which at least one  $^{18}\text{O}$ -labeled ASV belongs (at 21 or 98 days) are shown. Bars show the abundance in triplicate microcosms. (G) The relative 16S rRNA gene sequence abundance of  $^{18}\text{O}$ -labeled and unlabeled ASVs in the unfractionated libraries of replicate microcosms. Sixteen to 18% of the relative sequence abundance of the unfractionated libraries was not detected in the fractionated 98 day qSIP libraries. We attribute this "not detected" ASV abundance to community differences between biological replicates, and it is inherent in the qSIP method, which relies on comparison between biological replicates to determine AFE. The  $^{18}\text{O}$  incorporation status of ASVs of this "not detected" fraction cannot be determined, and so the relative abundances of these are not shown in the plot.

drop in oxygen concentrations or a detectable methanogen population in the 16S rRNA gene amplicon libraries. Thus, we have cautiously disregarded it. Despite the absence of obvious methane production or consumption, methanotrophs affiliated to *Methylocapsa* of the family *Beijerinckiaceae* and an unknown member of the *Methyloligellaceae* were  $^{18}\text{O}$ -labeled during the 21 day incubation. We also saw some evidence of the growth of aerobic methane oxidizers during the 98 day incubations, with notable labeling of the *pmoA* gene (Fig. 5B) which encodes the particulate methane monooxygenase enzyme that facilitates the conversion of methane to methanol during aerobic methane oxidation (98). The aggregate  $^{18}\text{O}$ -labeled *pmoA* gene DNA (yellow density peak  $\sim 1.710$  to  $\sim 1.730$  g mL $^{-1}$ , Fig. 5B) was of similar abundance to the aggregate non-labeled *pmoA* gene DNA (yellow density peak  $\sim 1.690$  g mL $^{-1}$ , Fig. 5B), indicating that up to half of the *pmoA*-containing cells grew during the 98 days following thaw.

No 16S rRNA gene amplicons affiliated with known methanotrophic clades were  $^{18}\text{O}$ -labeled at 98 days. Several members of the nitrite-reducing, methane-oxidizing Methyloirabilota were  $^{18}\text{O}$ -labeled after 21 days; however, all were affiliated with the non-methanotrophic Rokubacteriales, among which the *pmoA* gene has not been detected (99). None of the  $^{18}\text{O}$ -labeled ASVs affiliated with Verrucomicrobiota were affiliated with the methanotrophic clades of this phylum, which are *Methylacidiphilum* and *Methylacidimicrobium* (100). It is possible that growing methanotrophs (as detected by labeled *pmoA*-containing organisms) in 98 day incubations belonged to a clade or clades for which the methanotroph capability is not yet known. The PCR primers we used in this study are highly specific to the *pmoA* gene, unable to amplify closely related sequences such as *amoA*, the gene for ammonia oxidation (101). These primers will not amplify divergent *pmoA*-like genes such as those found in methane-oxidizing members of the Verrucomicrobiota and Methyloirabilota (102) or from novel taxa, and we therefore expect to have underestimated the true concentration of *pmoA*-like genes affiliated with methane oxidation. Many *pmoA*-containing microbial lineages have no cultured representatives (98, 103). The presence of  $^{18}\text{O}$ -labeled *pmoA* genes may alternatively suggest the growth of facultative methanotrophs that are able to grow on other carbon sources when methane is limiting, such as members of the *Methylocapsa* or the largely uncultured USCa group, which can use other C1 compounds such as methanol or acetate when methane is not readily available (104, 105). Methanotroph diversity is low in thawed permafrost-affected soils (106, 107), so the  $^{18}\text{O}$ -labeled *pmoA* DNA in our incubations might have derived from a low number of uncultivated *pmoA*-containing species. Methyloirabilota known to utilize methanol (a by-product of methane oxidation) and other C1 compounds were  $^{18}\text{O}$ -labeled during the 21 and 98 day incubations. These included *Bosea* sp. of the family *Beijerinckiaceae*, *Hyphomicrobium* sp. of the family *Hyphomicrobiaceae*, and *Methylotenera* sp. of the family *Methylophilaceae* (108).



**FIG 5** Density of *pmoA* genes extracted from  $\text{H}_2^{18}\text{O}$ -amended and  $\text{H}_2^{16}\text{O}$  control microcosms. The abundances of *pmoA* genes at different buoyant densities measured with qPCR at (A) 21 and (B) 98 days of oxidic incubation at  $4^\circ\text{C}$  are shown. Blue lines show the abundance of *pmoA* genes in DNA extracted from the microcosms that received  $\text{H}_2^{16}\text{O}$  water (i.e.,  $\text{H}_2^{16}\text{O}$  control). The yellow lines show the abundance of *pmoA* genes in DNA extracted from the microcosms that received  $\text{H}_2^{18}\text{O}$  water. The solid and dashed lines correspond to technical replicates. The y-axis values represent the percent of the *pmoA* gene abundances normalized to the maximum value within the same replicate.

### Microbial dormancy

Soils are regarded to harbor a diverse, yet low-abundance, dormant microbial community (109). In our microcosms, approximately half of the ASVs in thawed active layer soils remained unlabeled. These non-growing ASVs contributed  $27\% \pm 6\%$  (21 days) and  $29\% \pm 3\%$  (98 days) of the relative 16S rRNA gene sequence abundance. These non-growing ASVs were diverse and affiliated with many phyla. No ASVs associated with the phyla Cyanobacteria, Elusimicrobiota, Enttheonellaota, MBNT15, RCP2-54, Sumerlaeota, or WPS-2 were  $^{18}\text{O}$ -labeled at 21 or 98 days. Thus, despite these groups being present in the total community, we did not detect any growing organisms from these clades. The relative 16S rRNA gene sequence abundances of these same non-growing ASVs were abundant in parallel anoxic microcosms ( $30\% \pm 9\%$  at 21 days and  $35\% \pm 3\%$  at 98 days). We therefore suggest that the reason these ASVs did not grow during oxidic thaw at  $4^\circ\text{C}$  is a combination of different requirements specific to each clade and not simply because they required anoxic conditions for growth. These non-growing ASVs may require additional nutrients or other environmental characteristics not provided to them

by the soil, their immediate environment, or the conditions of the microcosm in order to grow. For example, certain microorganisms depend on the availability of biologically active trace elements (biometals, as defined by Giovannelli [110]) as cofactors for key biogeochemical reactions important in organic carbon degradation and overall carbon cycling (111). Physico-chemical factors including pH and the availability of key trace elements might restrain growth of certain groups or increase resource competition. Additionally, some microorganisms require trace quantities of the atmospheric gases H<sub>2</sub> or CO (112) which may not have been sufficiently available to them in the microcosm headspace.

Overall, this work highlights that cell dormancy, or very slow growth, contributes to the total microbial diversity of this subsurface active layer Arctic soil during thawing. Consideration of this dormant or slow-growing fraction in soil microbial-biogeochemical models will improve the mechanistic realism and predictions of carbon dynamics and emissions from soil on seasonal timescales (30, 113, 114) and is necessary for understanding biogeochemical transformations in dynamic environments such as seasonally variable Arctic systems (31). Should nutrients or environmental factors be encountered that promote the growth of dormant cells, rapid recruitment from this dormant population to the growing population may occur (72, 109). The physical connectivity across and throughout active layer soils potentially contributes to the transportation and dispersal of both nutrients and dormant cells (115).

Additionally, some of the unlabeled ASVs in this study may be dead (i.e., extracellular DNA (116) or necromass) or growing very slowly, such that growth cannot be detected over 98 days using qSIP. However, the impact of extracellular DNA on microbial community composition after 21 and 98 days of incubation is likely to be small owing to degradation of extracellular DNA associated with microbial necromass consumption and replacement of extracellular DNA with DNA from recently growing clades (117, 118). Overall, we found that active layer soils harbored both microorganisms that are primed to grow after soil thaw and others that form a seed bank and remain dormant, dead, or in a very slow mode of growth.

### Seasonality of Arctic soils and the impact of climate warming

About 28% of permafrost area in northern regions is likely to experience thaw if global warming stabilizes at 2°C above pre-industrial levels (119). Meanwhile, the mean thickness of the active layer in the northern polar region has increased by 0.11 cm per year between 2003 and 2020 due to thawing of underlying permafrost (6). Even under optimistic emissions scenarios, the global active layer soil volume is projected to significantly increase as Arctic permafrost thaws (13), causing a substantial amount of permafrost carbon to undergo seasonal thawing. The warming Arctic climate is also likely to cause an increase in the number of days per year that active layer soils experience temperatures above 0°C (10) (Fig. S8). We anticipate that, with the lengthening of the thawed period, the activity of “late”-growing microorganisms (here represented by those growing after 98 days of thaw) will become increasingly influential on carbon transformations and greenhouse gas emissions from permafrost-affected regions. The increase in taxonomic richness that we observed in the “late”-growing community may also equip soils with richer biogeochemical functions and metabolisms. For example, we found that the abundance of <sup>18</sup>O-labeled *pmoA* genes from growing microorganisms was higher in the “late”-growing community than the “early” communities (Fig. 5). Notably, we did not observe a corresponding increase in methane concentrations in our microcosms, suggesting that the “late”-growing community detected here may have oxidized any methane released from the thawed soil. Similarly, the lower degree of <sup>18</sup>O-labeling in *pmoA*-bearing microorganisms in the “early” community suggests that this community may be, compared to the “late”-growing community, relatively less prepared to oxidize trapped methane that is released following thawing of active layer or permafrost soils. The presence of growing microorganisms capable of methane oxidation is consistent with recent observations of net negative methane fluxes from the soil to the atmosphere

(i.e., methane uptake) in high Arctic tundra during the summer season in Svalbard (120) and northern Canada (121, 122).

## Changing hydrology

Our microcosm-based study did not account for dynamic hydrological regimes that may occur during natural seasonal thawing. Hydrological changes, including the inundation and draining of soil, may alter redox status and replenish carbon substrates and other nutrients, altering or enhancing rates of microbial activity, growth, and biogeochemical rates (123). For instance, methane oxidation may be enhanced in the drier portion of the summer in increasingly aerated soil (120). At our study site, observations show that soil moisture at 22 cm below the soil surface rises from ~8% (volume) to ~32% after thaw (44), potentially affecting microbial community structure and growth (124–127). In our microcosm experiments, the addition of H<sub>2</sub><sup>18</sup>O water to create slurries increased the liquid water content by ~5 times, potentially altering the post-thaw microbial community structure relative to *in situ* active layer soil. Nevertheless, our findings closely mirror *in situ* observations of the dominant phyla in active layer soil (68), supporting the relevance of our microcosm study to understanding active layer soil dynamics.

## Conclusions

High Arctic regions, including Svalbard, are among the fastest-warming places on Earth (36, 37). This warming is resulting in permafrost degradation and longer active layer thaw seasons. We used DNA qSIP with H<sub>2</sub><sup>18</sup>O (33) to trace taxon-specific growth following active layer thawing for 21 and 98 days. We revealed time-dependent microbial community dynamics, including distinct “early” and “late” stage growers, a notable prevalence of dormancy, and potential microbial predation, death, and turnover. Notable CO<sub>2</sub> production (attributed to the resumption of microbial activity) occurred within days of thawing, indicating that Arctic soil carbon is susceptible to microbial degradation during short-lived winter warming events when soil temperatures surpass 0°C (65). After 21 and 98 day incubations, approximately half of the diversity in active layer soil was attributed to microorganisms that did not measurably grow, underscoring the prevalence of dormancy even during thawed summer-like conditions and the value of carrying out physiology-based microbial assays for understanding microbial community dynamics in thawing Arctic soils. We found that bacterial predation and epibiosis are important factors shaping microbial community dynamics in seasonally thawed Arctic soils. We did not observe methane production or consumption, yet we detected a growing community that was primed for methane oxidation after thaw. Our study reveals that Arctic soils harbor a microbial community that undergoes complex growth, predation, and dormancy dynamics during seasonal thawing—processes that shape the seasonal population structure and regulate carbon storage dynamics. These high Arctic soil habitats are exceptionally vulnerable to warming and contemporary climate change, leading to further alterations of soil ecological dynamics and carbon cycling.

## ACKNOWLEDGMENTS

This work would not have been possible without the leadership of Tullis C. Onstott, a co-investigator of this project who passed away partway through the project's completion. We acknowledge the assistance of John Cliff of the Environmental Molecular Science Laboratory, Pacific National Laboratory, for funding acquisition. We also thank Natalie Ludgate and Thomas Kelly in the School of Geography at Queen Mary University of London for their expert technical input and guidance in this work. We are grateful to the staff of the Ny-Ålesund Research Station–Sverdrup, the UK Arctic Research Station, and the AWIPEV Arctic Research Base in Ny-Ålesund, Svalbard, for logistical support in the field.

This work was supported by funding from NERC (NE/T010967/1) (to J.A.B.), the European Research Council (ERC) under the European Union's Horizon Europe Research

and Innovation programme (grant agreement no. 101115755, acronym SIESTA) (to J.A.B.), the Agence Nationale de la Recherche (ANR23-CPJ1-0172-01) (to J.A.B.), and the Excellence Initiative of Aix-Marseille University–A\*MIDEX, a French "Investissements d'Avenir" programme. This work also received support from the Deutsche Forschungsgemeinschaft (Project OR 417/7-1) (to W.D.O.). This work also received financial support from the NERC COVID Recovery Support Fund administered by the British Antarctic Survey, the NERC Arctic Research Station Access Scheme (to J.A.B.), and the IHSS Seed-corn Fund at Queen Mary University of London (to J.A.B.). M.A.C., J.A.B., and W.D.O. acknowledge support from the Center for Advanced Studies (CAS Fellowship) at LMU Munich. M.A.C. acknowledges support from the Federation of European Microbiological Societies Research and Training Grant. K.G.L., A.D.S., T.A.V., and R.L.H. acknowledge support from the US Department of Energy, Office of Science, Office of Biological and Environmental Research, Genomic Science Program (DE-SC0020369). D.G. received support from the Italian Ministry of University and Research (MUR) through the Italian Arctic Research Program "Programma Ricerche in Artico (PRA)," project PRA2021-0014 "Impact of climate change-induced permafrost and ice melting on the biodiversity and ecosystem functioning of Arctic environments (Melting-ICE)," and the European Research Council (ERC) under the European Union's Horizon 2020 research and innovation program (grant number 948972-COEVOLVE-ERC-2020-STG).

#### AUTHOR AFFILIATIONS

<sup>1</sup>School of Geography, Queen Mary University of London, London, United Kingdom

<sup>2</sup>School of Biological and Behavioural Sciences, Queen Mary University of London, London, United Kingdom

<sup>3</sup>Department of Science, Natural History Museum, London, United Kingdom

<sup>4</sup>Department of Earth and Environmental Sciences, Paleontology & Geobiology, Ludwig-Maximilians-Universität München, Munich, Germany

<sup>5</sup>Department of Biology, University of Naples Federico II, Naples, Italy

<sup>6</sup>Department of Marine and Coastal Sciences, Rutgers University, New Brunswick, New Jersey, USA

<sup>7</sup>UK Centre for Ecology & Hydrology, Wallingford, United Kingdom

<sup>8</sup>Department of Earth and Planetary Sciences, University of Tennessee, Knoxville, Tennessee, USA

<sup>9</sup>Department of Microbiology, University of Tennessee, Knoxville, Tennessee, USA

<sup>10</sup>Biosciences Division, Oak Ridge National Laboratory, Oak Ridge, Tennessee, USA

<sup>11</sup>Kovda Institute of Physicochemical and Biological Problems in Soil Science, Russian Academy of Sciences, Pushchino, Russia

<sup>12</sup>Chilterns National Landscape, Chinnor, United Kingdom

<sup>13</sup>Permafrost Research, Alfred Wegener Institute Helmholtz Centre for Polar and Marine Research, Potsdam, Germany

<sup>14</sup>Geography Department, Humboldt-Universität of Berlin, Berlin, Germany

<sup>15</sup>Institute for Marine Biological Resources and Biotechnologies, Italian National Research Council, CNR-IRBIM, Ancona, Italy

<sup>16</sup>Earth-Life Science Institute, ELSI, Tokyo Institute of Technology, Tokyo, Japan

<sup>17</sup>Marine Chemistry and Geochemistry Department, Woods Hole Oceanographic Institution, Woods Hole, Massachusetts, USA

<sup>18</sup>Department of Biological Sciences, University of Southern California, Dornsife College of Letters, Arts and Sciences, Los Angeles, California, USA

<sup>19</sup>Department of Earth Sciences, University of Southern California, Dornsife College of Letters, Arts and Sciences, Los Angeles, California, USA

<sup>20</sup>GeoBio-Center LMU, Ludwig-Maximilians-Universität München, Munich, Germany

<sup>21</sup>Aix Marseille Univ, Université de Toulon, CNRS, IRD, MIO, Marseille, France

## AUTHOR ORCID*s*

Margaret A. Cramm  <http://orcid.org/0000-0003-3530-5560>

Ömer K. Coskun  <http://orcid.org/0009-0005-9786-5397>

Tatiana A. Vishnivetskaya  <http://orcid.org/0000-0002-0660-023X>

Robert L. Hettich  <http://orcid.org/0000-0001-7708-786X>

Andrew D. Steen  <http://orcid.org/0000-0003-4297-4332>

Karen G. Lloyd  <http://orcid.org/0000-0003-0914-6375>

William D. Orsi  <http://orcid.org/0000-0002-4094-5637>

Anne D. Jungblut  <http://orcid.org/0000-0002-4569-8233>

James A. Bradley  <http://orcid.org/0000-0003-3640-208X>

## FUNDING

Funder	Grant(s)	Author(s)
Natural Environment Research Council	NE/T010967/1	James A. Bradley
US Department of Energy, Office of Science, Office of Biological and Environmental Research, Genomic Science Program	DE-SC0020369	Karen G. Lloyd
Italian Ministry of University and Research, Italian Arctic Research Program	PRA2021-0014	Donato Giovannelli
HORIZON EUROPE European Research Council	948972-COEVOLVE-ERC-2020-STG	Donato Giovannelli
HORIZON EUROPE European Research Council	101115755	James A. Bradley
Agence Nationale de la Recherche	ANR23-CPJ1-0172-01	James A. Bradley
Deutsche Forschungsgemeinschaft	OR 417/7-1	William D. Orsi
British Antarctic Survey		James A. Bradley
Queen Mary University of London		James A. Bradley
Ludwig-Maximilians-Universität München Center for Advanced Studies		William D. Orsi
Federation of European Microbiological Societies		Margaret A. Cramm

## AUTHOR CONTRIBUTIONS

Margaret A. Cramm, Conceptualization, Data curation, Formal analysis, Funding acquisition, Investigation, Methodology, Project administration, Visualization, Writing – original draft, Writing – review and editing | Ömer K. Coskun, Investigation, Methodology, Visualization, Writing – review and editing | Francesco Montemagno, Investigation, Methodology, Writing – review and editing | Matteo Selci, Resources, Writing – review and editing | Tim Goodall, Data curation, Methodology, Writing – review and editing | Brianna Green, Resources, Writing – review and editing | Sayali A. Mulay, Resources, Writing – review and editing | Katie Sipes, Resources, Writing – review and editing | Andrey A. Abramov, Methodology, Resources, Writing – review and editing | Catherine M. Heppell, Supervision, Writing – review and editing | Julia Boike, Funding acquisition, Project administration, Writing – review and editing | Donato Giovannelli, Funding acquisition, Investigation, Resources, Writing – review and editing | Tatiana A. Vishnivetskaya, Funding acquisition, Investigation, Project administration, Resources, Writing – review and editing | Robert L. Hettich, Funding acquisition, Investigation, Project administration, Writing – review and editing | Andrew D. Steen, Funding acquisition, Investigation, Writing – review and editing | Karen G. Lloyd, Conceptualization, Funding acquisition, Investigation, Project administration, Resources, Writing – review and editing | William D. Orsi, Conceptualization, Investigation, Methodology, Project administration,

Resources, Supervision, Writing – review and editing | Anne D. Jungblut, Methodology, Supervision, Writing – review and editing | James A. Bradley, Conceptualization, Formal analysis, Funding acquisition, Investigation, Project administration, Resources, Supervision, Writing – original draft, Writing – review and editing, Writing – review and editing, Resources, Validation.

## DATA AVAILABILITY

DNA sequence data can be found in the NCBI Sequence Read Archive under the BioProject accession [PRJNA1118335](https://doi.org/10.1038/s41586-018-0371-0). Soil core and pit physical and geochemical data can be found in the Zenodo archive at <https://doi.org/10.5281/zenodo.19084687>.

## ADDITIONAL FILES

The following material is available [online](#).

### Supplemental Material

**Supplemental Information (mSystems00738-25-s0001.docx)**. Supplemental text, figures, and tables.

### Open Peer Review

**PEER REVIEW HISTORY (review-history.pdf)**. An accounting of the reviewer comments and feedback.

## REFERENCES

- Lindgren A, Hugelius G, Kuhry P. 2018. Extensive loss of past permafrost carbon but a net accumulation into present-day soils. *Nature* 560:219–222. <https://doi.org/10.1038/s41586-018-0371-0>
- Schuur EAG, Abbott BW, Commann R, Ernakovich J, Euskirchen E, Hugelius G, Grosse G, Jones M, Koven C, Leshyk V, Lawrence D, Lorant MM, Mauritz M, Olefeldt D, Natali S, Rodenhizer H, Salmon V, Schädel C, Strauss J, Treat C, Turetsky M. 2022. Permafrost and climate change: carbon cycle feedbacks from the warming arctic. *Annu Rev Environ Resour* 47:343–371. <https://doi.org/10.1146/annurev-environ-012220-011847>
- Rantanen M, Karpechko AY, Lipponen A, Nordling K, Hyvärinen O, Ruosteenoja K, Vihma T, Laaksonen A. 2022. The Arctic has warmed nearly four times faster than the globe since 1979. *Commun Earth Environ* 3:1–10. <https://doi.org/10.1038/s43247-022-00498-3>
- Harden JW, Koven CD, Ping C, Hugelius G, David McGuire A, Camill P, Jorgenson T, Kuhry P, Michaelson GJ, O'Donnell JA, Schuur EAG, Tarnocai C, Johnson K, Grosse G. 2012. Field information links permafrost carbon to physical vulnerabilities of thawing. *Geophys Res Lett* 39. <https://doi.org/10.1029/2012GL051958>
- Biskaborn BK, Smith SL, Noetzli J, Matthes H, Vieira G, Streletskiy DA, Schoeneich P, Romanovsky VE, Lewkowicz AG, Abramov A, et al. 2019. Permafrost is warming at a global scale. *Nat Commun* 10:264. <https://doi.org/10.1038/s41467-018-08240-4>
- Liu Z, Kimball JS, Ballantyne A, Watts JD, Natali SM, Rogers BM, Yi Y, Klene AE, Moghaddam M, Du J, Zona D. 2024. Widespread deepening of the active layer in northern permafrost regions from 2003 to 2020. *Environ Res Lett* 19:014020. <https://doi.org/10.1088/1748-9326/ad0f73>
- Schuur EAG, McGuire AD, Schädel C, Grosse G, Harden JW, Hayes DJ, Hugelius G, Koven CD, Kuhry P, Lawrence DM, Natali SM, Olefeldt D, Romanovsky VE, Schaefer K, Turetsky MR, Treat CC, Vonk JE. 2015. Climate change and the permafrost carbon feedback. *Nature* 520:171–179. <https://doi.org/10.1038/nature14338>
- Miner KR, Turetsky MR, Malina E, Bartsch A, Tamminen J, McGuire AD, Fix A, Sweeney C, Elder CD, Miller CE. 2022. Permafrost carbon emissions in a changing Arctic. *Nat Rev Earth Environ* 3:55–67. <https://doi.org/10.1038/s43017-021-00230-3>
- Nikrad MP, Kerkhof LJ, Häggblom MM. 2016. The subzero microbiome: microbial activity in frozen and thawing soils. *FEMS Microbiol Ecol* 92:1–16.
- Bruhwiller L, Parmentier F-J, Crill P, Leonard M, Palmer PI. 2021. The Arctic carbon cycle and its response to changing climate. *Curr Clim Change Rep* 7:14–34. <https://doi.org/10.1007/s40641-020-00169-5>
- Domeignoz-Horta LA, Pold G, Liu XJA, Frey SD, Melillo JM, DeAngelis KM. 2020. Microbial diversity drives carbon use efficiency in a model soil. *Nat Commun* 11:3684. <https://doi.org/10.1038/s41467-020-17502-z>
- Glassman SI, Weihe C, Li J, Albright MBN, Looby CI, Martiny AC, Treseder KK, Allison SD, Martiny JBH. 2018. Decomposition responses to climate depend on microbial community composition. *Proc Natl Acad Sci USA* 115:11994–11999. <https://doi.org/10.1073/pnas.1811269115>
- Chadburn SE, Burke EJ, Cox PM, Friedlingstein P, Hugelius G, Westermann S. 2017. An observation-based constraint on permafrost loss as a function of global warming. *Nature Clim Change* 7:340–344. <https://doi.org/10.1038/nclimate3262>
- Nauta AL, Heijmans MMPD, Blok D, Limpens J, Elberling B, Gallagher A, Li B, Petrov RE, Maximov TC, van Huissteden J, Berendse F. 2015. Permafrost collapse after shrub removal shifts tundra ecosystem to a methane source. *Nature Clim Change* 5:67–70. <https://doi.org/10.1038/nclimate2446>
- Roy Chowdhury T, Herndon EM, Phelps TJ, Elias DA, Gu B, Liang L, Wullschlegel SD, Graham DE. 2015. Stoichiometry and temperature sensitivity of methanogenesis and CO<sub>2</sub> production from saturated polygonal tundra in Barrow, Alaska. *Glob Chang Biol* 21:722–737. <https://doi.org/10.1111/gcb.12762>
- Singleton CM, McCalley CK, Woodcroft BJ, Boyd JA, Evans PN, Hodgkins SB, Chanton JP, Frolking S, Crill PM, Saleska SR, Rich VI, Tyson GW. 2018. Methanotrophy across a natural permafrost thaw environment. *ISME J* 12:2544–2558. <https://doi.org/10.1038/s41396-018-0065-5>
- Song X, Wang G, Ran F, Huang K, Sun J, Song C. 2020. Soil moisture as a key factor in carbon release from thawing permafrost in a boreal forest. *Geoderma* 357:113975. <https://doi.org/10.1016/j.geoderma.2019.113975>
- Song Y, Song C, Hou A, Sun L, Wang X, Ma X, Jiang L, Liu C, Gao J. 2021. Temperature, soil moisture, and microbial controls on CO<sub>2</sub> and CH<sub>4</sub> emissions from a permafrost peatland. *Environ Prog Sustain Energy* 40:e13693. <https://doi.org/10.1002/ep.13693>
- Treat CC, Natali SM, Ernakovich J, Iversen CM, Lupascu M, McGuire AD, Norby RJ, Roy Chowdhury T, Richter A, Šantrůčková H, Schädel C, Schuur EAG, Sloan VL, Turetsky MR, Waldrop MP. 2015. A pan-Arctic

- synthesis of CH<sub>4</sub> and CO<sub>2</sub> production from anoxic soil incubations. *Glob Change Biol* 21:2787–2803. <https://doi.org/10.1111/gcb.12875>
20. Yvon-Durocher G, Allen AP, Bastviken D, Conrad R, Gudasz C, St-Pierre A, Thanh-Duc N, del Giorgio PA. 2014. Methane fluxes show consistent temperature dependence across microbial to ecosystem scales. *Nature* 507:488–491. <https://doi.org/10.1038/nature13164>
  21. Baker CCM, Barker AJ, Douglas TA, Doherty SJ, Barbato RA. 2023. Seasonal variation in near-surface seasonally thawed active layer and permafrost soil microbial communities. *Environ Res Lett* 18:055001. <https://doi.org/10.1088/1748-9326/acc542>
  22. Schostag M, Stibal M, Jacobsen CS, Bælum J, Taş N, Elberling B, Jansson JK, Semenchuk P, Priemé A. 2015. Distinct summer and winter bacterial communities in the active layer of Svalbard permafrost revealed by DNA- and RNA-based analyses. *Front Microbiol* 6:399. <https://doi.org/10.3389/fmicb.2015.00399>
  23. Feng J, Wang C, Lei J, Yang Y, Yan Q, Zhou X, Tao X, Ning D, Yuan MM, Qin Y, Shi ZJ, Guo X, He Z, Van Nostrand JD, Wu L, Bracho-Garillo RG, Penton CR, Cole JR, Konstantinidis KT, Luo Y, Schuur EAG, Tiedje JM, Zhou J. 2020. Warming-induced permafrost thaw exacerbates tundra soil carbon decomposition mediated by microbial community. *Microbiome* 8:3. <https://doi.org/10.1186/s40168-019-0778-3>
  24. Müller O, Bang-Andreasen T, White RA, Elberling B, Taş N, Kneafsey T, Jansson JK, Øvreås L. 2018. Disentangling the complexity of permafrost soil by using high resolution profiling of microbial community composition, key functions and respiration rates. *Environ Microbiol* 20:4328–4342. <https://doi.org/10.1111/1462-2920.14348>
  25. Xue Y, Jonassen I, Øvreås L, Taş N. 2020. Metagenome-assembled genome distribution and key functionality highlight importance of aerobic metabolism in Svalbard permafrost. *FEMS Microbiol Ecol* 96:1–13. <https://doi.org/10.1093/femsec/fiaa057>
  26. Schostag M, Priemé A, Jacquioud S, Russel J, Ekelund F, Jacobsen CS. 2019. Bacterial and protozoan dynamics upon thawing and freezing of an active layer permafrost soil. *ISME J* 13:1345–1359. <https://doi.org/10.1038/s41396-019-0351-x>
  27. He Y, Yang J, Zhuang Q, Harden JW, McGuire AD, Liu Y, Wang G, Gu L. 2015. Incorporating microbial dormancy dynamics into soil decomposition models to improve quantification of soil carbon dynamics of northern temperate forests. *JGR Biogeosci* 120:2596–2611. <https://doi.org/10.1002/2015JG003130>
  28. Chandel AK, Jiang L, Luo Y. 2023. Microbial models for simulating soil carbon dynamics: a review. *JGR Biogeosciences* 128:e2023JG007436. <https://doi.org/10.1029/2023JG007436>
  29. Lennon JT, Abramoff RZ, Allison SD, Burckhardt RM, DeAngelis KM, Dunne JP, Frey SD, Friedlingstein P, Hawkes CV, Hungate BA, Khurana S, Kivlin SN, Levine NM, Manzoni S, Martiny AC, Martiny JBH, Nguyen NK, Rawat M, Talmy D, Todd-Brown K, Vogt M, Wieder WR, Zakem EJ. 2024. Priorities, opportunities, and challenges for integrating microorganisms into earth system models for climate change prediction. *mBio* 15:e00455–24. <https://doi.org/10.1128/mbio.00455-24>
  30. Lyu Z, Sommers P, Schmidt SK, Magnani M, Cimpoiasu M, Kuras O, Zhuang Q, Oh Y, De La Fuente M, Cramm M, Bradley JA. 2024. Seasonal dynamics of Arctic soils: capturing year-round processes in measurements and soil biogeochemical models. *Earth Sci Rev* 254:104820. <https://doi.org/10.1016/j.earscirev.2024.104820>
  31. Bradley JA. 2025. Microbial dormancy as an ecological and biogeochemical regulator on earth. *Nat Commun* 16:3909. <https://doi.org/10.1038/s41467-025-59167-6>
  32. Walz J, Knoblauch C, Böhme L, Pfeiffer E-M. 2017. Regulation of soil organic matter decomposition in permafrost-affected Siberian tundra soils - impact of oxygen availability, freezing and thawing, temperature, and labile organic matter. *Soil Biol Biochem* 110:34–43. <https://doi.org/10.1016/j.soilbio.2017.03.001>
  33. Hungate BA, Mau RL, Schwartz E, Caporaso JG, Dijkstra P, van Gestel N, Koch BJ, Liu CM, McHugh TA, Marks JC, Morrissey EM, Price LB. 2015. Quantitative microbial ecology through stable isotope probing. *Appl Environ Microbiol* 81:7570–7581. <https://doi.org/10.1128/AEM.02280-15>
  34. Propster JR, Schwartz E, Hayer M, Miller S, Monsaint-Queeney V, Koch BJ, Morrissey EM, Mack MC, Hungate BA. 2023. Distinct growth responses of tundra soil bacteria to short-term and long-term warming. *Appl Environ Microbiol* 89:e01543-22. <https://doi.org/10.1128/aem.01543-22>
  35. Purcell AM, Dijkstra P, Hungate BA, McMillen K, Schwartz E, van Gestel N. 2023. Rapid growth rate responses of terrestrial bacteria to field warming on the Antarctic Peninsula. *ISME J* 17:2290–2302. <https://doi.org/10.1038/s41396-023-01536-4>
  36. Adakudlu M, Andersen J, Bakke J, Beldring S, et al. 2019. Climate in Svalbard 2100 – a knowledge base for climate adaptation. Edited by I. Hanssen-Bauer, E. Førland, H. Hisdal, S. Mayer, A. B. Sandø, and A. Sorteberg. Norwegian Centre of Climate Services (NCCS) for Norwegian Environment Agency (Miljødirektoratet) NCCS report 1/2019. <https://doi.org/10.25607/OBP-888>
  37. Isaksen K, Nordli Ø, Ivanov B, Koltzow MAØ, Aaboe S, Gjelten HM, Mezghani A, Eastwood S, Førland E, Benestad RE, Hanssen-Bauer I, Brækkan R, Sviashchennikov P, Demin V, Revina A, Karandasheva T. 2022. Exceptional warming over the Barents area. *Sci Rep* 12:9371. <https://doi.org/10.1038/s41598-022-13568-5>
  38. Boike J, Juszak I, Lange S, Chadburn S, Burke E, Overduin PP, Roth K, Ippisch O, Bornemann N, Stern L, Gouttevin I, Hauber E, Westermann S. 2018. A 20-year record (1998–2017) of permafrost, active layer and meteorological conditions at a high Arctic permafrost research site (Bayvelva, Spitsbergen). *Earth Syst Sci Data* 10:355–390. <https://doi.org/10.5194/essd-10-355-2018>
  39. Boike J, Grünberg I, Miesner F, Bornemann N, Cable WL. 2022. Continuous measurements in soil and air at the permafrost long-term observatory at the Bayvelva station near Ny-Ålesund (2018 et seq) [dataset bundled publication]. PANGAEA.
  40. Shi T, Reeves RH, Gilichinsky DA, Friedmann EI. 1997. Characterization of viable bacteria from Siberian permafrost by 16S rDNA sequencing. *Microb Ecol* 33:169–179. <https://doi.org/10.1007/s002489900019>
  41. Montemagno F, Cascone M, Cardellini C, Pasotti J, Manini E, Baldrighi E, Maiero E, Segato D, Cerrato R, Mazzola M, Vardè M, Cordone A, Caliro S, Rudnik I, Cramm M, Bradley JA, Giovannelli D. 2024. PRA melting-ICE project: svalbard 2022 expeditions report. *Open Res Eur* 4:257. <https://doi.org/10.12688/openreseurope.17772.1>
  42. Blazewicz SJ, Schwartz E. 2011. Dynamics of. *Microb Ecol* 61:911–916. <https://doi.org/10.1007/s00248-011-9826-7>
  43. Trejos-Espeleta JC, Marin-Jaramillo JP, Schmidt SK, Sommers P, Bradley JA, Orsi WD. 2024. Principal role of fungi in soil carbon stabilization during early pedogenesis in the high Arctic. *Proc Natl Acad Sci USA* 121:e2402689121. <https://doi.org/10.1073/pnas.2402689121>
  44. Grünberg I, Groenke B, Westermann S, Boike J. 2024. Permafrost and active layer temperature and freeze/thaw timing reflect climatic trends at Bayvelva, Svalbard. *JGR Earth Surface* 129:e2024JF007648. <https://doi.org/10.1029/2024JF007648>
  45. Coskun ÖK, Pichler M, Vargas S, Gilder S, Orsi WD. 2018. Linking uncultivated microbial populations and benthic carbon turnover by using quantitative stable isotope probing. *Appl Environ Microbiol* 84:e01083-18. <https://doi.org/10.1128/AEM.01083-18>
  46. Neufeld JD, Vohra J, Dumont MG, Lueders T, Manefield M, Friedrich MW, Murrell JC. 2007. DNA stable-isotope probing. *Nat Protoc* 2:860–866. <https://doi.org/10.1038/nprot.2007.109>
  47. Cramm MA. 2023. Understanding microbial activity with isotope labelling of DNA. *Nat Rev Earth Environ* 4:142–142. <https://doi.org/10.1038/s43017-023-00394-0>
  48. Apprill A, McNally S, Parsons R, Weber L. 2015. Minor revision to V4 region SSU rRNA 806R gene primer greatly increases detection of SAR11 bacterioplankton. *Aquat Microb Ecol* 75:129–137. <https://doi.org/10.3354/ame01753>
  49. Parada AE, Needham DM, Fuhrman JA. 2016. Every base matters: assessing small subunit rRNA primers for marine microbiomes with mock communities, time series and global field samples. *Environ Microbiol* 18:1403–1414. <https://doi.org/10.1111/1462-2920.13023>
  50. Tavormina PL, Ussler W 3rd, Orphan VJ. 2008. Planktonic and sediment-associated aerobic methanotrophs in two seep systems along the North American margin. *Appl Environ Microbiol* 74:3985–3995. <https://doi.org/10.1128/AEM.00069-08>
  51. Steinberg LM, Regan JM. 2008. Phylogenetic comparison of the methanogenic communities from an acidic, oligotrophic fen and an anaerobic digester treating municipal wastewater sludge. *Appl Environ Microbiol* 74:6663–6671. <https://doi.org/10.1128/AEM.00553-08>
  52. Cramm MA, Neves B de M, Manning CCM, Oldenburg TBP, Archambault P, Chakraborty A, Cyr-Parent A, Edinger EN, Jaggi A, Mort A, Tortell P, Hubert CRJ. 2021. Characterization of marine microbial communities around an Arctic seabed hydrocarbon seep at Scott Inlet, Baffin Bay. *Sci Total Environ* 762:143961. <https://doi.org/10.1016/j.scitotenv.2020.143961>

53. Martin M. 2011. Cutadapt removes adapter sequences from high-throughput sequencing reads. *EMBnet j* 17:10. <https://doi.org/10.14806/fej.17.1.200>
54. Callahan BJ, McMurdie PJ, Rosen MJ, Han AW, Johnson AJA, Holmes SP. 2016. DADA2: High-resolution sample inference from Illumina amplicon data. *Nat Methods* 13:581–583. <https://doi.org/10.1038/nmeth.3869>
55. Lee MD. 2019. Happy Belly Bioinformatics: an open-source resource dedicated to helping biologists utilize bioinformatics. *JOSE* 2:53. <https://doi.org/10.21105/jose.00053>
56. Quast C, Pruesse E, Yilmaz P, Gerken J, Schweer T, Yarza P, Peplies J, Glöckner FO. 2013. The SILVA ribosomal RNA gene database project: improved data processing and web-based tools. *Nucleic Acids Res* 41:D590–6. <https://doi.org/10.1093/nar/gks1219>
57. Wang Q, Garrity GM, Tiedje JM, Cole JR. 2007. Naive Bayesian classifier for rapid assignment of rRNA sequences into the new bacterial taxonomy. *Appl Environ Microbiol* 73:5261–5267. <https://doi.org/10.1128/AEM.00062-07>
58. Oren A. 2024. On validly published names, correct names, and changes in the nomenclature of phyla and genera of prokaryotes: a guide for the perplexed. *NPJ Biofilms Microbiomes* 10:20. <https://doi.org/10.1038/s41522-024-00494-9>
59. R Core Team. 2023. R: a language and environment for statistical computing. R Foundation for Statistical Computing, Vienna, Austria.
60. Oksanen J, Blanchet FG, Kindt R, Legendre P, Minchin PR, Hara RBO, Simpson GL, Solymos P, Stevens MHH. 2014. Package “vegan”
61. McMurdie PJ, Holmes S. 2013. Phyloseq: an R package for reproducible interactive analysis and graphics of microbiome census data. *PLoS One* 8:e61217. <https://doi.org/10.1371/journal.pone.0061217>
62. Coskun ÖK, Özen V, Wankel SD, Orsi WD. 2019. Quantifying population-specific growth in benthic bacterial communities under low oxygen using H218O. *ISME J* 13:1546–1559. <https://doi.org/10.1038/s41396-019-0373-4>
63. Youngblut ND, Barnett SE, Buckley DH. 2018. HTSSIP: an R package for analysis of high throughput sequencing data from nucleic acid stable isotope probing (SIP) experiments. *PLoS One* 13:e0189616. <https://doi.org/10.1371/journal.pone.0189616>
64. Sieradzki ET, Koch BJ, Greenlon A, Sachdeva R, Malmstrom RR, Mau RL, Blazewicz SJ, Firestone MK, Hofmocker KS, Schwartz E, Hungate BA, Pett-Ridge J. 2020. Measurement error and resolution in quantitative stable isotope probing: implications for experimental design. *mSystems* 5:e00151-20. <https://doi.org/10.1128/mSystems.00151-20>
65. Bradley JA, Molares Moncayo L, Gallo G, Brusca J, Vignezio T, Pasotti J, Giovannelli D. 2025. Svalbard winter warming is reaching melting point. *Nat Commun* 16:6409. <https://doi.org/10.1038/s41467-025-6092-6-8>
66. Megonigal JP, Hines ME, Visscher PT. 2003. Anaerobic metabolism: linkages to trace gases and aerobic processes, p 317–424. In Holland HD, Turekian KK (ed), *Treatise on geochemistry*. Pergamon, Oxford.
67. Gittel A, Bárta J, Kohoutová I, Schneckler J, Wild B, Capek P, Kaiser C, Torsvik VL, Richter A, Schleper C, Urlich T. 2014. Site- and horizon-specific patterns of microbial community structure and enzyme activities in permafrost-affected soils of Greenland. *Front Microbiol* 5:541. <https://doi.org/10.3389/fmicb.2014.00541>
68. Loganathachetti DS, Venkatachalam S, Jabir T, Vipindas PV, Krishnan KP. 2022. Total nitrogen influence bacterial community structure of active layer permafrost across summer and winter seasons in Ny-Ålesund, Svalbard. *World J Microbiol Biotechnol* 38:28. <https://doi.org/10.1007/s11274-021-03210-3>
69. Mujakić I, Piwosz K, Koblížek M. 2022. Phylum gemmatimonadota and its role in the environment. *Microorganisms* 10:151. <https://doi.org/10.3390/microorganisms10010151>
70. Strous M, Fuerst JA, Kramer EHM, Logemann S, Muyzer G, van de Pas-Schoonen KT, Webb R, Kuenen JG, Jetten MSM. 1999. Missing lithotroph identified as new planctomycete. *Nature* 400:446–449. <https://doi.org/10.1038/22749>
71. Basan M, Honda T, Christodoulou D, Hörl M, Chang Y-F, Leoncini E, Mukherjee A, Okano H, Taylor BR, Silverman JM, Sanchez C, Williamson JR, Paulsson J, Hwa T, Sauer U. 2020. A universal trade-off between growth and lag in fluctuating environments. *Nature* 584:470–474. <https://doi.org/10.1038/s41586-020-2505-4>
72. Bradley JA, Trivedi CB, Winkel M, Mourot R, Lutz S, Larose C, Keuschnig C, Doting E, Halbach L, Zervas A, Anesio AM, Benning LG. 2023. Active and dormant microorganisms on glacier surfaces. *Geobiology* 21:244–261. <https://doi.org/10.1111/gbi.12535>
73. Kvernvik AC, Hoppe CJM, Lawrenz E, Prášil O, Greenacre M, Wiktor JM, Leu E. 2018. Fast reactivation of photosynthesis in arctic phytoplankton during the polar night<sup>1</sup>. *J Phycol* 54:461–470. <https://doi.org/10.1111/jpy.12750>
74. Gudelj I, Weitz JS, Ferenci T, Claire Horner - Devine M, Marx CJ, Meyer JR, Forde SE. 2010. An integrative approach to understanding microbial diversity: from intracellular mechanisms to community structure. *Ecol Lett* 13:1073–1084. <https://doi.org/10.1111/j.1461-0248.2010.01507.x>
75. Jørgensen BB, Marshall IPG. 2016. Slow microbial life in the seabed. *Ann Rev Mar Sci* 8:311–332. <https://doi.org/10.1146/annurev-marine-010814-015535>
76. Bird JT, Tague ED, Zinke L, Schmidt JM, Steen AD, Reese B, Marshall IPG, Webster G, Weightman A, Castro HF, Campagna SR, Lloyd KG. 2019. Uncultured microbial phyla suggest mechanisms for multi-thousand-year subsistence in Baltic Sea sediments. *mBio* 10:e02376-18. <https://doi.org/10.1128/mBio.02376-18>
77. Buckeridge KM, Mason KE, McNamara NP, Ostle N, Puissant J, Goodall T, Griffiths RI, Stott AW, Whitaker J. n.d. Environmental and microbial controls on microbial necromass recycling, an important precursor for soil carbon stabilization. *Commun Earth Environ* 1. <https://doi.org/10.1038/s43247-020-00031-4>
78. Herrmann A, Witter E. 2002. Sources of C and N contributing to the flush in mineralization upon freeze–thaw cycles in soils. *Soil Biol Biochem* 34:1495–1505. [https://doi.org/10.1016/S0038-0717\(02\)00121-9](https://doi.org/10.1016/S0038-0717(02)00121-9)
79. Wu X, Spencer S, Gushgari-Doyle S, Yee MO, Voriskova J, Li Y, Alm EJ, Chakraborty R. 2020. Culturing of “unculturable” subsurface microbes: natural organic carbon source fuels the growth of diverse and distinct bacteria from groundwater. *Front Microbiol* 11. <https://doi.org/10.3389/fmicb.2020.610001>
80. Ho A, Lonardo DPD, Bodelier PLE. 2017. Revisiting life strategy concepts in environmental microbial ecology. *Microbiol Ecol* 93:fx006. <https://doi.org/10.1093/femsec/fix006>
81. Fierer N, Leff JW, Adams BJ, Nielsen UN, Bates ST, Lauber CL, Owens S, Gilbert JA, Wall DH, Caporaso JG. 2012. Cross-biome metagenomic analyses of soil microbial communities and their functional attributes. *Proc Natl Acad Sci USA* 109:21390–21395. <https://doi.org/10.1073/pnas.1215210110>
82. Larsbrink J, McKee LS. 2020. Bacteroidetes bacteria in the soil: Glycan acquisition, enzyme secretion, and gliding motility. *Adv Appl Microbiol* 110:63–98. <https://doi.org/10.1016/bs.aambs.2019.11.001>
83. Mendes-Soares H, Velicer GJ. 2013. Decomposing predation: testing for parameters that correlate with predatory performance by a social bacterium. *Microb Ecol* 65:415–423. <https://doi.org/10.1007/s00248-012-0135-6>
84. Scheel M, Zervas A, Rijkers R, Tveit AT, Ekelund F, Campuzano Jiménez F, Christensen TR, Jacobsen CS. 2023. Abrupt permafrost thaw triggers activity of copiotrophs and microbiome predators. *FEMS Microbiol Ecol* 99:fiad123. <https://doi.org/10.1093/femsec/fiad123>
85. Petters S, Groß V, Söllinger A, Pichler M, Reinhard A, Bengtsson MM, Urlich T. 2021. The soil microbial food web revisited: Predatory myxobacteria as keystone taxa? *ISME J* 15:2665–2675. <https://doi.org/10.1038/s41396-021-00958-2>
86. He X, McLean JS, Edlund A, Yooseph S, Hall AP, Liu S-Y, Dorrestein PC, Esquenazi E, Hunter RC, Cheng G, Nelson KE, Lux R, Shi W. 2015. Cultivation of a human-associated TM7 phylotype reveals a reduced genome and epibiotic parasitic lifestyle. *Proc Natl Acad Sci USA* 112:244–249. <https://doi.org/10.1073/pnas.1419038112>
87. Wang Y, Zhang Y, Hu Y, Liu L, Liu S-J, Zhang T. 2023. Genome-centric metagenomics reveals the host-driven dynamics and ecological role of CPR bacteria in an activated sludge system. *Microbiome* 11:56. <https://doi.org/10.1186/s40168-023-01494-1>
88. Lemos LN, Medeiros JD, Dini-Andreote F, Fernandes GR, Varani AM, Oliveira G, Pylro VS. 2019. Genomic signatures and co-occurrence patterns of the ultra-small *Saccharimonadia* (phylum CPR/Patescibacteria) suggest a symbiotic lifestyle. *Mol Ecol* 28:4259–4271. <https://doi.org/10.1111/mec.15208>
89. Chen H, Athar R, Zheng G, Williams HN. 2011. Prey bacteria shape the community structure of their predators. *ISME J* 5:1314–1322. <https://doi.org/10.1038/ismej.2011.4>
90. Chen H, Young S, Berhane T-K, Williams HN. 2012. Predatory bacteriovorax communities ordered by various prey species. *PLoS One* 7:e34174. <https://doi.org/10.1371/journal.pone.0034174>

91. Lovering AL, Sockett RE. 2021. Microbe Profile: Bdellovibrio bacteriovorus: a specialized bacterial predator of bacteria. *Microbiology* 167:001043. <https://doi.org/10.1099/mic.0.001043>
92. Waite DW, Chuvochina M, Pelikan C, Parks DH, Yilmaz P, Wagner M, Loy A, Naganuma T, Nakai R, Whitman WB, Hahn MW, Kuever J, Hugenholtz P. 2020. Proposal to reclassify the proteobacterial classes *Deltaproteobacteria* and *Oligoflexia*, and the phylum *Thermodesulfobacteria* into four phyla reflecting major functional capabilities. *Int J Syst Evol Microbiol* 70:5972–6016. <https://doi.org/10.1099/ijsem.0.004213>
93. Hungate BA, Marks JC, Power ME, Schwartz E, van Groenigen KJ, Blazewicz SJ, Chuckran P, Dijkstra P, Finley BK, Firestone MK, et al. 2021. The functional significance of bacterial predators. *mBio* 12:e00466-21. <https://doi.org/10.1128/mBio.00466-21>
94. Bautista MA, Zhang C, Whitaker RJ. 2015. Virus-induced dormancy in the archaeon *Sulfolobus islandicus*. *mBio* 6:e02565-14. <https://doi.org/10.1128/mBio.02565-14>
95. Rengefors K, Karlsson I, Hansson L. 1998. Algal cyst dormancy: a temporal escape from herbivory. *Proc R Soc Lond B* 265:1353–1358. <https://doi.org/10.1098/rspb.1998.0441>
96. Lennon JT, den Hollander F, Wilke-Berenguer M, Blath J. 2021. Principles of seed banks and the emergence of complexity from dormancy. *Nat Commun* 12:4807. <https://doi.org/10.1038/s41467-021-24733-1>
97. Schwartz DA, Shoemaker WR, Mägälie A, Weitz JS, Lennon JT. 2023. Bacteria-phage coevolution with a seed bank. *ISME J* 17:1315–1325. <https://doi.org/10.1038/s41396-023-01449-2>
98. Knief C. 2015. Diversity and habitat preferences of cultivated and uncultivated aerobic methanotrophic bacteria evaluated based on pmoA as molecular marker. *Front Microbiol* 6. <https://doi.org/10.3389/fmicb.2015.01346>
99. Ivanova AA, Oshkin IY, Danilova OV, Philippov DA, Ravin NV, Dedys SN. 2021. Rokubacteria in northern peatlands: habitat preferences and diversity patterns. *Microorganisms* 10:11. <https://doi.org/10.3390/microorganisms10010011>
100. Schmitz RA, Peeters SH, Versantvoort W, Picone N, Pol A, Jetten MSM, Op den Camp HJM. 2021. Verrucomicrobial methanotrophs: ecophysiology of metabolically versatile acidophiles. *FEMS Microbiol Rev* 45:fuab007. <https://doi.org/10.1093/femsre/fuab007>
101. Costello AM, Lidstrom ME. 1999. Molecular characterization of functional and phylogenetic genes from natural populations of methanotrophs in lake sediments. *Appl Environ Microbiol* 65:5066–5074. <https://doi.org/10.1128/AEM.65.11.5066-5074.1999>
102. Luesken FA, Zhu B, van Alen TA, Butler MK, Diaz MR, Song B, Op den Camp HJM, Jetten MSM, Ettwig KF. 2011. pmoA primers for detection of anaerobic methanotrophs. *Appl Environ Microbiol* 77:3877–3880. <https://doi.org/10.1128/AEM.02960-10>
103. Dumont MG, Lüke C, Deng Y, Frenzel P. 2014. Classification of pmoA amplicon pyrosequences using BLAST and the lowest common ancestor method in MEGAN. *Front Microbiol* 5:1–11. <https://doi.org/10.3389/fmicb.2014.00034>
104. Danilova OV, Oshkin IY, Belova SE, Miroshnikov KK, Ivanova AA, Dedys SN. 2023. One step closer to enigmatic usca methanotrophs: isolation of a *Methylocapsa*-like bacterium from a subarctic soil. *Microorganisms* 11:2800. <https://doi.org/10.3390/microorganisms11112800>
105. Dedys SN, Khmelenina VN, Suzina NE, Trotsenko YA, Semrau JD, Liesack W, Tiedje JM. 2002. *Methylocapsa acidiphila* gen. nov., sp. nov., a novel methane-oxidizing and dinitrogen-fixing acidophilic bacterium from sphagnum bog. *Int J Syst Evol Microbiol* 52:251–261. <https://doi.org/10.1099/00207713-52-1-251>
106. Tveit A, Schwacke R, Svenning MM, Urlich T. 2013. Organic carbon transformations in high-Arctic peat soils: key functions and microorganisms. *ISME J* 7:299–311. <https://doi.org/10.1038/ismej.2012.99>
107. Tveit AT, Urlich T, Svenning MM. 2014. Metatranscriptomic analysis of arctic peat soil microbiota. *Appl Environ Microbiol* 80:5761–5772. <https://doi.org/10.1128/AEM.01030-14>
108. Chistoserdova L. 2015. Methylotrophs in natural habitats: current insights through metagenomics. *Appl Microbiol Biotechnol* 99:5763–5779. <https://doi.org/10.1007/s00253-015-6713-z>
109. Lennon JT, Jones SE. 2011. Microbial seed banks: the ecological and evolutionary implications of dormancy. *Nat Rev Microbiol* 9:119–130. <https://doi.org/10.1038/nrmicro2504>
110. Giovannelli D. 2023. Trace metal availability and the evolution of biogeochemistry. *Nat Rev Earth Environ* 4:597–598. <https://doi.org/10.1038/s43017-023-00477-y>
111. Hay Mele B, Monticelli M, Leone S, Bastoni D, Barosa B, Cascone M, Migliaccio F, Montemagno F, Ricciardelli A, Tonietti L, Rotundi A, Cordone A, Giovannelli D. 2023. Oxidoreductases and metal cofactors in the functioning of the earth. *Essays Biochem* 67:653–670. <https://doi.org/10.1042/EBC20230012>
112. Greening C, Grinter R. 2022. Microbial oxidation of atmospheric trace gases. *Nat Rev Microbiol* 20:513–528. <https://doi.org/10.1038/s41579-022-00724-x>
113. Salazar A, Lennon JT, Dukes JS. 2019. Microbial dormancy improves predictability of soil respiration at the seasonal time scale. *Biogeochemistry* 144:103–116. <https://doi.org/10.1007/s10533-019-00574-5>
114. Zha J, Zhuang Q. 2020. Microbial dormancy and its impacts on northern temperate and boreal terrestrial ecosystem carbon budget. *Biogeosciences* 17:4591–4610. <https://doi.org/10.5194/bg-17-4591-2020>
115. Mestre M, Höfer J. 2021. The microbial conveyor belt: connecting the globe through dispersion and dormancy. *Trends Microbiol* 29:482–492. <https://doi.org/10.1016/j.tim.2020.10.007>
116. Carini P, Marsden PJ, Leff JW, Morgan EE, Strickland MS, Fierer N. 2016. Relic DNA is abundant in soil and obscures estimates of soil microbial diversity. *Nat Microbiol* 2:16242. <https://doi.org/10.1038/nmicrobiol.2016.242>
117. Lennon JT, Muscarella ME, Placella SA, Lehmkuhl BK. 2018. How, when, and where relic DNA affects microbial diversity. *mBio* 9:e00637-18. <https://doi.org/10.1128/mBio.00637-18>
118. Santos-Medellin C, Blazewicz SJ, Pett-Ridge J, Firestone MK, Emerson JB. 2023. Viral but not bacterial community successional patterns reflect extreme turnover shortly after rewetting dry soils. *Nat Ecol Evol* 7:1809–1822. <https://doi.org/10.1038/s41559-023-02207-5>
119. Liu L, Zhao D, Wei J, Zhuang Q, Gao X, Zhu Y, Zhang J, Guo C, Zheng D. 2021. Permafrost sensitivity to global warming of 1.5 °C and 2 °C in the Northern Hemisphere. *Environ Res Lett* 16:034038. <https://doi.org/10.1088/1748-9326/abd6a8>
120. Donato A, Famulari D, Giovannelli D, Mariani A, Mazzola M, Decesari S, Pappacoglio G. 2024. Observations of methane net sinks in the Arctic tundra. *EGUosphere*. <https://doi.org/10.5194/eguosphere-2024-1440>
121. Voigt C, Virkkala A-M, Hould Gosselin G, Bennett KA, Black TA, Detto M, Chevrier-Dion C, Guggenberger G, Hashmi W, Kohl L, Kou D, Marquis C, Marsh P, Marushchak ME, Nestic Z, Nykänen H, Saarela T, Sauheitl L, Walker B, Weiss N, Wilcox EJ, Sonnentag O. 2023. Arctic soil methane sink increases with drier conditions and higher ecosystem respiration. *Nat Clim Chang* 13:1095–1104. <https://doi.org/10.1038/s41558-023-01785-3>
122. Lau MCY, Stackhouse BT, Layton AC, Chauhan A, Vishnivetskaya TA, Chourey K, Ronholm J, Myktyczuk NCS, Bennett PC, Lamarche-Gagnon G, Burton N, Pollard WH, Omelon CR, Medvigy DM, Hettich RL, Pfiffner SM, Whyte LG, Onstott TC. 2015. An active atmospheric methane sink in high arctic mineral cryosols. *ISME J* 9:1880–1891. <https://doi.org/10.1038/ismej.2015.13>
123. Waldrop MP, Ernakovich JG, Vishnivetskaya TA, Schaefer SR, Mackelprang R, Barta J, O'Brien JM, Winkler M, Barbato RA, Heffernan L, et al. 2025. Microbial ecology of permafrost soils: populations, processes, and perspectives. *Permafrost Periglacial* 36:245–258. <https://doi.org/10.1002/ppp.2264>
124. Blazewicz SJ, Schwartz E, Firestone MK. 2014. Growth and death of bacteria and fungi underlie rainfall-induced carbon dioxide pulses from seasonally dried soil. *Ecology* 95:1162–1172. <https://doi.org/10.1890/13-1031.1>
125. Meisner A, Snoek BL, Nesme J, Dent E, Jacquiod S, Classen AT, Priemé A. 2021. Soil microbial legacies differ following drying-rewetting and freezing-thawing cycles. *ISME J* 15:1207–1221. <https://doi.org/10.1038/s41396-020-00844-3>
126. Sokol NW, Slessarev E, Marschmann GL, Nicolas A, Blazewicz SJ, Brodie EL, Firestone MK, Foley MM, Hestrin R, Hungate BA, Koch BJ, Stone BW, Sullivan MB, Zablocki O, LLNL Soil Microbiome Consortium, Pett-Ridge J. 2022. Life and death in the soil microbiome: how ecological processes influence biogeochemistry. *Nat Rev Microbiol* 20:415–430. <https://doi.org/10.1038/s41579-022-00695-z>
127. Sipes K, Buongiorno J, Steen AD, Abramov AA, Abua C, Peters SL, Gianonne RJ, Hettich RL, Boike J, Garcia SL, Vishnivetskaya TA, Lloyd KG. 2024. Depth-specific distribution of bacterial MAGs in permafrost active layer in Ny Ålesund, Svalbard (79°N). *Syst Appl Microbiol* 47:126544. <https://doi.org/10.1016/j.syapm.2024.126544>